HYDROGEN SELECTIVE PROPERTIES OF CESIUM-HYDROGENSULPHATE MEMBRANES

FAIEK MEYER

A thesis submitted in partial fulfilment of the requirements for the degree of Magister Scientiae in the Department of Chemistry

University of the Western Cape

Supervisor: Prof. V.M. Linkov

Co-supervisor Dr. B.J. Bladergroen

November 2006

HYDROGEN SELECTIVE PROPERTIES OF CESIUM-HYDROGENSULPHATE MEMBRANES

FAIEK MEYER

KEYWORDS:

Cesium hydrogensulphate

Hydrogen separation membrane

Idea selectivity

Gas permeance

Permeation mechanism

Proton conductivity

Phase characterization

ABSTRACT:

HYDROGEN SELECTIVE PROPERTIES OF CESIUM-HYDROGENSULPHATE MEMBRANES

FAIEK MEYER

M.Sc Thesis, department of Chemistry, University of the Western Cape

The production procedure of a $CsHSO_4$-SiO_2 composite membrane was optimized in order to obtain the highest possible H_2:CO_2 and H_2:CH_4 Idea selectivity permeance. The optimized membrane preparation procedure led to the preparation of membranes with Idea selectivity of 5 and 10 towards H_2:CH_4 and H_2:CO_2 respectively. The H_2 permeance value is on average 0.15 $\mu mol \cdot s^{-1} \cdot m^{-2} \cdot Pa^{-1}$. The reproducibility of the optimized membrane was further investigated and was found to be satisfactory. An attempt was made to discover the gas transport mechanism of H_2, CH_4 and CO_2. Gas permeance measurements were carried out as a function of time and temperature (between 25-180°C) using H_2, CH_4 and CO_2 as analyte gases. XRD, TGA and impedance spectroscopy were used to identify the phases of $CsHSO_4$ within the membrane. The gas permeation mechanism was found to be a combination of Knudsen diffusion and solution diffusion. The pores that allow Knudsen diffusion (allow transport of H_2, CH_4 and CO_2) are believed to be located at the $CsHSO_4$ crystal phase boundaries. In parallel, H_2 diffuses selectively through the lattice of phase II/III of $CsHSO_4$. .

DECLARATION

I declare that *HYDROGEN SELECTIVE PROPERTIES OF CESIUM HYDROGENSULPHATE MEMBRANES* is my own work, that it has not been submitted before for any degree or examination in any other university, and that all the sources I have used or quoted have been indicated and acknowledged by complete references.

Faiek Meyer November 2006

Signed:……

ACKNOWLEDGEMENTS:

I firstly would like to thank Allah, for granting me the honour to study what He has created. I would like to thank my supervisor, Prof Vladimir Linkov and Co-supervisor, Dr Ben Bladergroen for the patients, assistance and expertise offered during the research. I would also like to offer a special thanks to SAIAMC for their time and analytical support. I was privileged to be part of multi-skilled laboratory personnel who were always willing. A special word of thanks to my friends Rushanah Fakir, Wafeeq Davids, Hanna and Salam for their support. Thank you Mario Williams for editing my thesis. Finally, the unconditional families support, which I certainly would not have being able to do without.

TABLE OF CONTENTS:

LIST FIGURES:

LIST OF TABLES:

1 INTRODUCTION:

The annual demand for hydrogen by chemical industries has risen to 500 billion Nm^3 with an increasing growth rate of 10-15% [1,2]. The demand is likely to increase significantly in the near future due to the interest of hydrogen as a fuel in fuel cells. Hydrogen is one of the most abundantly produced and consumed gases in industry and plays a vital role in production of various chemicals, particularly ammonia (i.e. the Haber-Bosch process which consumes 50% of the hydrogen produced worldly), and the petroleum and petrochemical industries, which consume 35-45% of H_2 for hydrogenation and desulphurisation of crude feed stocks [6,22]. A smaller but still significant amount of hydrogen is used in other industries such as methanol production, space operations (i.e. rocket fuel) and fine chemical industries.

Hydrogen is currently produced by recovery technologies incorporated in various chemical processes. Hydrogen is mainly sourced from fossil fuels via steam reformation and coal gasification [2]. Both processes will be discussed in section 1.1. Special attention will be given to Underground Coal Gasification since it may be of great importance for the future of South Africa. In section 1.2, the issues related to the separation of H_2 from syngas will be discussed. The problem statement and the aim of the study will be highlighted in section 1.3.

1.1 H_2 PRODUCTION:

1.1.1 Steam reformation

Steam reformation is the most common method for the production of hydrogen and accounts for 80% of the global hydrogen economy [2]. It is the most understood and least expensive procedure in hydrogen production. Steam reformation is a process, which converts alkanes, more commonly methane, into hydrogen; carbon dioxide; and carbon monoxide by the use of steam. Steam reformation involves a three-step process to produce hydrogen. Methane is firstly catalytically reformed at elevated temperature and pressure to produce a syngas mixture of H_2 and CO. The water shift reaction is then catalytically carried out to combine CO and H_2O to produce the H_2 product and CO_2. At this stage the hydrogen recovery process is implemented. The reforming step is illustrated in the following reaction:

$$\mathbf{CH_4 + H_2O \rightarrow 2H_2 + CO \quad \Delta H = +206\ kJ/mol} \qquad \mathbf{[1]}$$

This reaction is endothermic due to the positive change in enthalpy as indicated above (Equation 1). The reforming reaction is carried out in a reformer containing tubes filled with nickel catalyst at temperatures between 700ºC and 1000ºC and a pressure around 30 atmospheres [3]. To prevent deactivation of the nickel catalyst, the methane feed passes through guard beds filled with zinc oxide or activated carbon to remove sulphur. An excess of steam is used to enhance conversion and to prevent thermal cracking and coking via the nickel-catalyzed Boudouard reaction:

$$\mathbf{2\ CO \rightarrow CO_2 + C \quad \Delta H = -172\ kJ/mol} \qquad \mathbf{[2]}$$

The excess steam also promotes the second step in the process, the so-called "water gas shift reaction", where the syngas is further converted to H_2 and CO_2 gases as illustrated in Equation 3:

$$\mathbf{CO + H_2O \rightarrow CO_2 + H_2} \qquad \mathbf{\Delta H = -41\ kJ/mol} \qquad \mathbf{[3]}$$

The water gas shift is typically carried out at a lower temperature than the reforming reaction. An iron-based catalyst may be used for higher temperature shifts (350ºC), and a copper based catalyst for lower shifts (205ºC)[4].

The third step, purification, is conventionally accomplished by pressure swing adsorption (PSA) to remove H_2O, CH_4, CO_2, N_2, and CO, from the H_2. After extraction of the H_2 product gas, the process gas may be treated to further remove CO_2 if sequestration is desired.

1.1.2 Coal gasification

Coal gasification is the oldest industrial process used for hydrogen production. It is generally more expensive to produce hydrogen from coal than from natural gas. This is due to the ratio of hydrogen to carbon, which in natural gas is 4:1 and coal is 0.8:1[4]. However, South Africa happens to have access to cheap coal which makes the production of H_2 from coal economically feasible. Coal gasification converts coal into H_2, CO_2, CH_4, H_2S, H_2O, CO and other organic compounds. Coal gasification is similar to steam reformation in that it also involves a three step process. The feedstock is treated at high temperature to produce a syngas followed by catalytic shift conversion.

In the first step of coal gasification (Equation 4), coal feedstock is broken down by high-pressure steam at 1300ºC to produce raw synthetic gas, as follows:

$$\textbf{Coal (carbon source)} + H_2O \rightarrow H_2 + CO \qquad [4]$$

The gasification step, requires heat and controlled addition of O_2, which allows partial oxidation of a small amount of the coal feedstock. This reaction is carried out in either a air-blown or oxygen-blown gasifier. Introducing nitrogen into the reactor increases the size and cost of the downstream equipment and makes separation of CO_2 much more difficult and costly.

In the second step (Equation 5), the syngas passes through a shift reactor converting most of the carbon monoxide to carbon dioxide, as shown in the reaction below:

$$CO + H_2O \rightarrow CO_2 + H_2 \qquad [5]$$

The shift reactor is adiabatic, operates at temperatures around 450ºC, and contains a sulphur-tolerant cobalt molybdate shift catalyst. The shifted syngas contains 60% volume hydrogen mixed with primarily CO_2 and some residual CO [5]. CH_4, O_2, N_2 and H_2S may also exist as impurities depending on the composition of the feed coal. The mixture is cooled and enters a lower temperature shift reactor, after which it is cooled again. In the third step, the H2 product is purified. Physical absorption removes 99% of H_2S impurities. The majority of H_2 in the shifted syngas (85%) is then removed as H_2 in a PSA unit [3].

1.1.3 Underground coal gasification:

World coal reserves are more abundant than the reserves of oil and natural gas together. Until the time that H_2 is produced by renewable energy sources, coal will most likely be the main feedstock for the production of H_2. However, it should be noted that the lion share of coal (75% in South Africa) cannot be mined economically using conventional methods. Moreover, the quality of the remaining 25% coal reserves is not very impressive. High ash and sulphur content of coal reduce the overall efficiency of the coal gasification process even further. However, the technology of underground coal gasification (UCG) has the potential to put H_2 produced from coal right back into the list of modern feasible hydrogen production technologies.

UCG is a proven technology that gasifies coal underground to producing gases and alkenes. UCG presents the ability to extract coal that would otherwise be un-mineable. It can utilize coal at great depths or in geologically difficult areas. With the current advancements in drilling technology, UCG will be more economical than the conventional mining processes since the mining cost are limited to drilling relatively small shafts. Significant cost savings are made since mine-workers (including their salaries and cost associated with safety issues) are no longer needed. Moreover, close to 100% of the coal seems can be gasified in comparison with the 40-60% in conventional mining. There are a few advantages for the environment as well: (a) the UCG sites are virtually unaffected by the mining operation and (b) the problems associated with ash-dumps are no longer relevant since the bulk of the ash remains underground. Theoretically, wastewater containing any type of organic residue can be

used as feedstock for UCG. Something that is not desirable is gasification above the ground since it could form deposits at the inside of the capital-intensive reactors.

The UCG process operates similarly to coal gasification and steam reformation in the utilization of air and steam. In UCG an injection well is prepared under the firth, by drilling vertically for depth, followed by horizontal drilling throughout the entire coal seem. A flexible stainless steel pipe is then inserted into the drilled column. The coal is ignited when steam and air are pumped down. This is the start of the syngas production process, the syngas containing H_2O, CH_4, CO_2, N_2, CO, H_2, H_2S and alkenes. The product gas is then led out of reaction zone through stainless steel piping. The gas finally reaches the surface where is will be used directly as fuel or as a source of H_2. The next section will discuss the possible complications related to the extraction of H_2 from the reaction mixture.

1.2 HYDROGEN SEPARATION

The final step in the chemical process entails the recovery of the desired products, in this case hydrogen. There are various ways in which hydrogen can be separated from the undesired products in the chemical processes. Steam reformation, coal gasification and UCG require an efficient H_2 recovery technique. Such a technique will lead to an increase in the profitability of supplying the hydrogen economy [19]. The current benchmark technology for H2 separation from gas mixtures containing high volumes of CO2 is Pressure Swing Adsorption (PSA). This technology will be discussed in section 1.2.1.

1.2.1 Pressure Swing Adsorption (PSA)

Currently, pressure swing adsorption (PSA) is the industrial technique that is widely applied over a vast range of chemical industries for the recovery of H_2 from other products [7].

The disadvantage of this process is that PSA is only efficient when the gas stream contains a relatively high percentage of H_2 relative to other gases. The H_2 content after the shift conversion in a steam reforming configuration is around 60%, high enough for the economical recovery of H_2. In the case where coal gasification is used, the hydrogen content decreases to <50 vol% with a large increase in the volume S, CH_4 and CO_2 [4]. As a result H_2 recovery is less economical leading to the increasing cycles of adsorption and desorption and inadequate H_2 separation [7].

When UCG is performed using air the H_2 content could drop below 10% in volume. Oxygen or enriched air can be considered as feedstock for UCG to boost the H2 content. However, this will lead to a significant cost increase of the gasification process. Alternatively, one should look at other gas separation technologies. Theoretically it would be more efficient to use membranes instead of PSA as a technique of recovery [1]. Membrane technology is a good candidate because of its ability separate continuously, low cost and maintenance and low energy consumption.

1.3 PROBLEM STATEMENT

Section 1.1 indicated the enormous need for H_2. Section 1.1.3 mentioned the enormous potential of UCG as modern economically feasible hydrogen production technology. Section 1.2 points out that the separation of H_2 from a UCG product gas mixture requires a highly permeable membrane with significant Idea selectivity towards H_2

As discussed in Chapter 2, the palladium membrane is the most investigated H_2 separation membrane and in some cases, utilized in industry. Palladium membranes are frequently mentioned in conjunction with steam reforming processes in the configuration of membrane reactors [50]. The advantage of such a configuration is that H_2 can be extracted from the reaction zone through the wall of a palladium film reactor [8], which will cause a desired shift of the reforming reaction equilibrium. Simultaneously, high purity hydrogen is obtained.

For UCG product gas, this advantage is not relevant since the reaction zone is deep underground. The UCG product gas is roughly 200ºC when it exits the earth. This is not particularly an optimum temperature for a Pd membranes and just too high for any polymer membrane.

The problem is that to date there is no commercially available membrane material with adequate properties to separate H_2 from a mixture of CO_2, CO, N_2 and CH_4 at 200ºC.

1.3.1 Hypothesis

The main aim of the study is to develop low temperature $CsHSO_4/SiO_2$ composite membranes that show significant Idea selectivity towards H_2:CO_2 and H_2:CH_4. The main focus of the research in membrane technology in this area includes the following sub-objectives:

- Optimising $CsHSO_4/SiO_2$ membrane preparation conditions for H_2 separation.
- Determination of the transport mechanism of hydrogen separation.
- Characterization of the membranes via XRD, IR, impedance spectroscopy and TGA.

1.3.2 Scope of thesis:

The investigation underway will be limited to H_2 properties of $CsHSO_4$ membranes and some other analyte gases (CH_4, CO_2) as a comparison. The respective membrane will be investigate as follows:

- Single gas permeability measurement will be used in the permeance measurements.
- Optimisation of the membrane preparation procedure and permselectivty of the relevant membranes.
- Gas permeance of $NaHSO_4$ membrane at room temperature.
- Gas permeance of membrane as a function of temperature
- Gas permeance of membrane as a function of time
- Effect of analyte gases on membranes.
- Identification of $CsHSO_4$, $NaHSO_4$ via IR

- Phase analysis of membrane using XRD, TGA and Impedance.
- Identification of transport mechanism.

1.3.3 Delimitations.

- $RbHSO_4$, CsH_2PO_4, $KHSO_4$ material and respective membranes couldn't be analysed due to time constrains
- Further investigation of the $CsHSO_4$ will be limited to the optimized membrane.
- Analysis of H_2S, alkanes, N_2 gases will not be done due to time constrains.
- Analysis of membrane by means of Raman spectroscopy. This instrument is not available in the Western Cape
- Analysis of phase as a function of temperature via XRD with a heating stage was not investigated. Itemba labs have started to upgrade their XRD facilities which will allow these type of measurements, however the heating stage is still not available due to several delays
- Mix gas analysis were not investigated due to time constrains

2 LITERATURE REVIEW

Over the past 40 years, research pertaining to membrane technology has lead to the development of a wide range of applications including beverage production, water purification and the separation of dairy products [22]. For the separation of gases, membrane technology is not as widely applied since the production of suitable gas separation membranes is far more challenging than the production of membranes for eg water purification. However, due to technological advances, more and more gas separating membranes have recently entered the market.

UCG, as discussed in section 1.1.3 is of great research interest for South Africa. This is due to the large coal reserves which South Africa possesses, of which 75% cannot be mine by conventional mining. UCG technology offers an inexpensive source of H_2, large enough to feed the H_2 hungry chemical industry (500 billion Nm^3 annually, growth rate 12-15% [3]) and potentially the even bigger H_2 economy market for many years. These facts create an enormous market potential for low-medium temperature H_2 separation techniques.

PSA is the current separation technology of choice in the industrial separation of hydrogen from gas streams [7]. However, it is well known that this process is inadequate for the separation of H_2 from low concentration hydrogen syngas (H_2, CO_2, CH_4, H_2S) streams. Membrane technology has been identified as an attractive alternative for

hydrogen separation from gas streams in combination with PSA or as a primary hydrogen separation system.

This literature review is meant to identify a membrane with significant Idea selectivity (above Knudsen selectivity) towards hydrogen and appropriate permeance at a temperatures around 200ºC.

Section 2.1 is an introduction to membrane technology, whereas section 2.2 focuses on membranes for gas separation, the most common materials employed, membrane classification and transport mechanisms. At the end of section 2.2 an overview will be given to identify the most promising membrane that can be applied for the separation of hydrogen from UCG product gas.

2.1 MEMBRANE TECHNOLOGY:

A membrane can be defined as a selective barrier between two phases. Membranes can divided into natural and synthetic membrane. The latter can be subdivided into organic and inorganic membranes, which can further be classified by structure and morphology.

This section will discuss the classification of membranes according to pore size in section 2.1.1, which will consider Microfiltration in section 2.1.1.1, Ultrafiltration in section 2.1.1.2 and Nanofiltration discussed in section 2.1.1.3.

2.1.1 **Classification of membranes according to pore size**:

Membranes are classified according to their pore size and can be divided into macroporous, mesoporous and microporous membranes as illustrated in table 1. The classification of the membrane often demarks its application in the filtration sector. Microporous and dense membranes are of great interest in this thesis. Note that the classification of the membrane does not differentiate between organic, inorganic, asymmetric or symmetric membranes.

Table 1: Definition of a type of filtration belonging to a particular pore size according to IUPAC

Terminology	Pore diameter (nm)	Types of filtration
Macroporous	$d_p > 50$	Microfiltration
Mesoporous	$2 < d_p < 50$	Ultrafiltration
Microporous	$d_p < 2$	Nano filtration and gas separation
Dense	No pores	Gas separation

2.1.1.1 Microfiltration:

A micro-filtration membrane is a blockade, which is driven by pressure gradient, to suspended solids and bacteria to produce water with improved purity. It is also used as pre-treatment for surface water, seawater, and biologically treated municipal effluent before other membrane systems. Applications include: drinking water, irrigation and industrial water reuse and makeup water [49].

2.1.1.2 Ultrafiltration:

Ultra-filtration (UF) is a pressure-driven barrier to suspended solids, bacteria, viruses, endotoxins and other pathogens to produce water with very high purity and low silt density. It serves as a pre-treatment for surface water, seawater, and biologically treated municipal effluent before reverse osmosis and other membrane systems. General Electric ultra-filtration membranes are supplied with molecular weight cut-offs (MWCO) from 13 000 to 200 000 Daltons [22].

2.1.1.3 Nanofiltration:

Nanofiltration is used when low molecular weight solutes such as inorganic salts or small organic membranes have to be separated from other solvents. It is a unique filtration process in-between Ultra Filtration and Reverse Osmosis, designed to achieve highly specific separations of low molecular weight compounds such as sugars from dissolved minerals and salts and gases. Typical applications include de-ashing of dairy products, recovery of hydrolyzed proteins, concentration of sugars and purification of soluble dyes, pigments and gas separation

2.1.1.4 Gas separation:

As can be seen in Table 1, gas separation can be achieved with microporous and dense membranes. The gas transport mechanisms for both classes of membranes, organic and inorganic, will be discussed in the following section.

2.2 MEMBRANES FOR GAS SEPARATION:

Micro porous and dense membranes will be discussed separately in section 2.2.1 and 2.2.2 respectively. Both sections have a subsection on the gas transport mechanism and show some examples from the literature. Section 2.2.3 is devoted to composite membranes.

2.2.1 **Micro porous membrane**:

Porous membranes are defined as void-like matrices, with structures of interconnected straight or complex pores. These membranes are generally characterized by high permeability but low selectivity. Porous inorganic membranes that have pore sizes greater than 0.3nm usually work as sieves for large molecules and particles [15]. Examples of these types of membranes used commercially are: Glass, alumina, zirconia, zeolite and carbon. They vary greatly in pore size, support material and configuration.

Inorganic microporous membranes can be subdivided into amorphous or crystalline types. Zeolites are a proper example of crystalline microporous inorganic membranes while silica is an example of the amorphous type [17]. The mechanism by which the membrane allows separation and permeation is described in the section below.

2.2.1.1 Transport mechanism in micro porous membranes

Three types of mechanisms bring about the separations of gases. The diffusion of molecules through the membrane in some cases involves just one mechanism but this is

not always the case because more complex combinational mechanisms can take place. These mechanisms are the Knudsen diffusion, surface diffusion and molecular sieves [26]. These mechanisms are discussed below.

Knudsen diffusion:

An important mechanism for the selective permeation of a gas through a porous ceramic membrane is Knudsen diffusion. Knudsen diffusion is the transport of gas molecules through a membrane in which the mean free path of the gas molecules is larger than the pore size of the membrane and as a result there is a greater frequency of collisions between gas molecules and pores wall compared to those strictly between gas molecules. Separation by this mechanism is achieved by the understanding that differently sized gas molecules or atoms move at different velocities. The selectivity of this separation mechanism is generally very low due to its ability to only separate gases with large differences in their molecular weights 58]. In addition, Knudsen diffusion is independent of the applied pressure as can be observed in the Knudsen equation:

$$D_k = 0.66\ r\ [(8\ R\ T) / (\pi\ M_W)]^{½}$$

where, D_k = Knudsen diffusion coefficient

T = temperature

M_W = molecular weight

R = universal gas constant (8.314 $J.K^{-1}.mol^{-1}$)

r = pore radius

At atmospheric pressure the mean free path of gases (A) is in the region of 100-200nm. For Knudsen flow to predominate in a selective membrane with pore radius (r), A/r must be greater than 5 and therefore the pores of the membrane must be less than 50nm [38]. The Knudsen flow of a gas through the membrane is proportional to the partial pressure difference of that gas across the membrane. The separation factor based on Knudsen separation is proportional to the square root of the molecular weight ratio of the gases, and is given by:

$$\alpha = \sqrt{\frac{M_2}{M_1}}$$

The principle is based on the fact that lighter molecule move faster than heavier molecules. Selectivity, however, is limited and can be calculated with the square root of the ratio of the molar masses of gases involved. For a Knudsen number <1, the dominant transportation mechanism is viscous flow, which is non selective.

Surface diffusion:

Surface diffusion occurs when gas molecules are adsorbed on the pore walls of the membranes and migrate along the surface. Surface diffusion increases the permeability of the component adsorbing more strongly to the membrane pores. At the same time, the effective pore diameter is reduced. Consequently, transport of non-adsorbing components is reduced and the selectivity is increased. The contribution of the surface diffusion towards the overall permeability is most pronounced at relative low temperatures, generally below 150ºC.

Molecular sieving:

Molecular sieves are used as a mechanism to separate that has different kinetic diameters. This separation can take place with sufficiently small pores sizes in the range of 3.0-5.3Å]

2.2.1.2 Examples of micro porous membranes:

This section discusses the following micro porous membranes; amorphous and crystalline.

Amorphous micro porous membranes:

Amorphous micro porous membranes are usually made of alumina, titania, zirconia or silica. These membranes are manufactured by a combination of a metal with a non-metal in the form of an oxide, nitride or carbide. Porous ceramic membranes generally have two layers; the top layer, which is usually a thin selective layer with small pores and a supporting membrane, which consist of large pores and in some cases an intermediate layer is required. When separation of gases is mainly by size exclusion, microporous membranes play an important role as a separating media**.** The intermediate layer helps to bridge the gap between the larger pore bottom layer and the smaller pore top layer.

Depending on the gas to be separated, the selectivity can reach up to 140, with promising hydrogen flux. Operating temperature for porous ceramic membranes is within the range of 200-600°C.

Smid *et al*. prepared ceramic hollow fibre membranes out of aluminium-oxide and silicon-nitride [15]. The hollow fibres are microporous and show gas flues of about 4-$1.4 \cdot 10^{-7}$ $cm^3 \cdot cm^{-2} \cdot s^{-1} \cdot Pa^{-1}$ and are selective to gases. The selectivity is close to the value predicted by the Knudsen diffusion theory. So it is possible to produce a defect free ceramic composite hollow fibre membrane. This membrane can serve as a basis for a highly selective membrane.

Sea *et al*., have produced a silica membrane, which was formed by chemical vapour deposition using tetraethylorthosilicate in the macropores of α-alumina or γ-alumina film coated on the α-alumina tube [62]. The reactant was evacuated through the porous wall, and silica was deposited in the macropores at 600-700°C. When the silica membrane was formed in a γ -alumina film coated on the α-alumina tube, hydrogen permeance at a temperature of 600°C was $3 \cdot 10^{-1}$ $\mu mol \cdot m^{-2} \cdot s^{-1} \cdot Pa^{-1}$, which was one order of magnitude higher than that of a membrane formed directly on the α-alumina tube. H_2/N_2 selectivity determined from the permeance of each component was 100-1000. The membrane formed in the γ -alumina film at 650°C showed a hydrogen permeance of $3 \cdot 10^{-2}$ $\mu mol \cdot m^{-2} \cdot s^{-1} \cdot Pa^{-1}$.

Crystalline micro porous membranes:

Zeolites are microporous crystalline alumino-silicates, having cage-like structures of particular geometry with Ångstrom-size pores of uniform shape. Thus, zeolite membranes have the potential to selectively separate mixtures of molecules [9]. Zeolites can act as molecular sieves and can be used for separating gas mixtures. Zeolite membranes have higher mechanical strength and greater thermal and chemical stability than polymeric membranes. These membranes consist of a thin continuous zeolitic layer composed of intergrown crystals on a porous support, which provides mechanical strength [48]. However, the production of defect free zeolite layer is challenging. To date zeolite membranes have not been made very successfully for hydrogen separation from other light gases [32].

Lin *et al*. reported high separation selectivities for a variety of mixtures using different types of zeolite membranes [22]. Most studies used MFI-type zeolites such as silicalite-1 (pure silica) and ZSM-5 (containing Al). These zeolites have both straight (0.54nm × 0.56nm) and sinusoidal (0.51nm × 0.54nm) channels, as measured by X-ray diffraction. If some molecules in a mixture are too large to enter the pores, separation can be obtained by molecular sieving. If both components in the feed permeate, then separation can be obtained due to differences in adsorption coverage, diffusion rates or the ability of one component in the feed to inhibit others from entering the pores.

Noble *et al*, prepared two different types of zeolite membrane that have been silicated [52]. One being the medium pore MFI membranes with a ten-membered ring structure

and the other being a small pore SAPO-34 membrane with an eight-membered ring structure. The H_2/CO_2 ideal selectivity can be as high as 235 for the silicated MFI membranes as compared to only 1.8 for the original membrane. The H_2 permeance however, decreased more than an order of magnitude. For H_2/CO_2, and H_2/CH_4 binary mixture separations, the MFI membrane was selective towards H_2 in the entire temperature range explored and furthermore the membrane became more promising at higher temperatures, as the H_2 permeance as well as separation selectivity increased as a function of temperature [52]. For SAPO-34 membranes, the silane precursor compound did not penetrate into the zeolite pores due to the small pore size. So only the pore entrance area and the bigger non-zeolite defects were affected. As a result, hydrogen permeance was almost unchanged after silylation. The H_2/CO_2 separation selectivity was unchanged. In terms of MFI-type zeolite membranes, the silane precursor compound could penetrate into the medium-sized zeolite pores. Thus after silylation, the zeolite pores were partially blocked resulting in a higher hydrogen selectivity towards other light gases.

2.2.2 Dense membranes

Non-porous or dense membranes are membranes that show no traces of voids in their structure [22]. The following three main types of dense membranes can be identified; organic, metallic and perovskite. The organic membranes show generally low permeability [23]. This is mainly due to the low solubility of the gases in the membrane material. The limited temperature range and the low selectivity towards H_2:CO_2 excludes the organic membrane from feasible application for the separation of H_2 from syngas.

Contrary to organic membranes, metallic and perovskite membranes show very high H_2 selectivity. The most important feature of these types of membranes is that it is possible to separate different molecules of similar molecular size (i.e. nitrogen and oxygen). The permeability of dense membranes becomes feasible for industry when the membrane thickness is reduced to values around 1μm. Various techniques (electroplating and CVD etc) have been investigated to produce thin films. Porous supports are used to provide the mechanical strength [49]. The separation mechanism can be described by solution diffusion and ion conduction which are discussed in the following section.

2.2.2.1 Transport mechanism in dense membranes

Two types of mechanisms bring about the separations of gases in membranes. These mechanisms are solution diffusion and ion conduction and are discussed below.

Solution diffusion:

The common mechanism used to describe the mode of gas transportation through dense metallic membranes is solution diffusion. The solution diffusion mechanism operates by adsorption of gases on the selective side of the dense membrane material, with diffusion taking place through the membrane in the form of atoms, which indicates the requirement of molecule splitting. The atoms then recombine at the other side of the membrane following desorption [22]. The permeability of dense membranes is generally proportional to the square root of the pressure.

Ion conduction:

Fast-ionic conductors are materials with high ionic conductivity in the solid state. These materials are of considerable commercial value because of their potential application in the construction of solid state batteries and fuel cells. This technological importance has provided the motivation for studies of both their structure and their dynamics, with the aim of enhancing our understanding of the conduction mechanism and determining important factors for the production of better ionic conductors. Structural studies have shown that these materials often exhibit extensive disordering of the mobile ions amongst interstitial sites in the crystal structure, providing further evidence of the ionic nature of the conduction. Hydrogen and Oxygen travel as ions (H_2 as H^+ and O_2 as O^{-2}) through the membrane [22]. The extent of the observed disorder and the energy barriers associated with hopping between the interstitial sites can be calculated from the measured conductivity.

2.2.2.2 Examples of dense membranes

This section will mainly discuss Pd-based membranes since this is the most widely investigated membrane for the separation of hydrogen from syngas.

Pd membranes:

Palladium membranes were first identified as highly hydrogen permeable membranes in the 19th century [23]. At that time palladium membrane was seen as a superior membrane

for hydrogen separation due to its catalytic surface, high hydrogen permeability and selectivity, thermal stability and corrosion resistance.

Itoh *et al,* have proposed a new method of preparing composite type palladium membrane for hydrogen separation [65]. Under optimum electroplating conditions, it was observed, that a thin layer of palladium with a thickness of several micrometers was densely packed inside the pores. The ideal separation factor for hydrogen and nitrogen was found to be more than 1000 above 300°C. However they are not economically viable due to its operational conditions. The temperature, at which the selectivity is satisfactory, is at 1000ºC, which is seen as the optimal temperature. The main problem with Pd membrane and most metal membrane is hydrogen embrittlement [8].

H_2 embrittlement is experienced by Palladium due to the transition from the α-phase to the β-phase. The phase transition from the α-β phase occurs at a temperature and hydrogen pressure below 571K and 2000kPa, respectively The relative decrease in selectivity and increase in permeability is due to lattice expansion at the phase transition point increasing in volume by about 10% [6]. This cell unit change can result in mechanical strain and physical distortion causing the underlying problem. Currently the most effective way to avoid the phase transformation (hydrogen embrittlement) problem is to use Ag alloyed Pd thin films, and to control the operation under such conditions (hydrogen pressure and temperature) that the phase transformation is avoided.

Pd alloy

The first group of dense inorganic membranes studied extensively in the past decade are metallic membranes, and primarily palladium alloy membranes (e.g Pd-Ag, Pd-Ni, Pd-Cu) for hydrogen separation . Recent studies were focused on the synthesis of supported thin metallic membranes, with a thickness ranging from the submicron to a few tens of microns, and their properties and applications. The research on the synthesis of thin metal-alloy membranes was motivated by the fact that the thin films can offer several advantages including reduced material costs, improved mechanical strength, increased tolerance to surface poisoning, and possibly higher hydrogen flux, compared to pure Pd membranes.

The three primary methods that have been developed to coat thin metal films on porous supports are electroless plating, chemical vapour deposition (CVD) and physical sputtering [12]. The two chemical methods (electroless plating and CVD) have the advantages of ease to scale up and flexibility to coat metal film on supports of different geometry. The main disadvantage of these methods is the difficulty to control the composition of metal alloy deposited.

Xomeritakis *et al,* have proposed a thin film (1-5μm) Pd/Ag membrane, supported on a sol–gel derived mesoporous alumina support [9]. Chemical vapour deposition and sputter coating was used to coat the ceramic support. The hydrogen permeance and H_2:He selectivity was in the range of 1.0^{-5}-2.0 $\mu mol.m^{-2}.s^{-1}Pa^{-1}$ and 20-200 at 300ºC, respectively.

Nam *et al,* proposed the preparation of a thin film dense palladium/nickel (Pd/Ni) alloy composite membrane, which is supported on mesoporous stainless steel. When the current density applied in vacuum electro-deposition is 6.5 mA/cm^2, the hydrogen permeance of the membrane fabricated was 0.0678 $\mu mol.m^{-2}.s^{-1}Pa^{-1}$ and hydrogen/nitrogen (H_2/N_2) selectivity was 3000 at 723K [48].

Palladium and palladium alloy membrane constitute a large percentage of the hydrogen selective membranes used in industry. However because palladium membranes are economically unviable due to their high cost, low permeability and hydrogen embrittlement, research interest has branched off into other metallic materials. Due to their meta-stable structure, amorphous alloy materials demonstrate high tenacity [8], freedom from hydrogen embrittlement as well as high hydrogen diffusivity, which identifies them as promising materials.

Hara *et al* have produced a 30mm thick amorphous $Zr_{36}Ni_{64}$ membrane, which was produced by rapid quenching [20]. The membrane was found to be tough in a hydrogen atmosphere and selective to hydrogen only. After exposing both sides of the membrane to a reactive gas, such as hydrogen and oxygen, the membrane exhibited a practical level of permeation rate more than 1 $cm^3/cm^2.min^{-1}$ H_2 at STP without noble metal coating.

The use of these membranes is limited due to the high cost of plant equipment, maintenance and low permeability. The permeability is even an order of magnitude smaller than that of palladium membranes.

2.2.3 Composite membranes

Membranes that incorporate different natural materials or synthetic materials are called composites of these materials [23]. Synthetic membranes or composites may be formed by use of organic and inorganic materials, comprising of a single morphological structure, or asymmetric consisting of two or more structural constituents with different morphologies. Symmetric membranes consist of a single chemical composition and structural morphology and may be classified into homogeneous, cylindrical porous or sponge-like porous kinds. An asymmetric membrane consists of more than one material with different morphology and may be differentiated into porous, integrally skinned or composite types. In the case were a single layer is deposited onto porous supports from a solution, a composite membrane may be formed. In some other membrane cases, supports are employed to form self-supported symmetric membrane, where it is either removed or forms an integral part of an asymmetric membrane or non-selective composite. Examples of such supports includes alumina, zirconia, titania, Vycor glass etc. The other motivation behind development of composite membrane is to incorporate the different material properties (i.e organic and inorganic) exhibited by the individual natural or synthetic materials in order to improve the properties of the existing membranes. Usually, the incorporation of inorganic material in organics is mainly associated with improvement of the thermal stability of the latter.

Bladergroen *et al*, has proposed a $CsHSO_4/SiO_2$ membrane [1]. The composite membrane was initially pressed between Pt containing current collectors and showed a selectivity of

4 and 8 for H_2:CH_4 and H_2:CO_2 respectively. When the composite membrane was measured without the Pt catalyst load, it showed a higher H_2 permeance of 1.0 x 10^{-1} – 1.5x 10^{-1} μmol.m^{-2}.$s^{-1}$$Pa^{-1}$, CH_4 permeance of 3.0 x 10^{-2} – 2.5x 10^{-2} μmol.m^{-2}.$s^{-1}$$Pa^{-1}$and a CO_2 permeance 1.0 x 10^{-2} – 1.5x 10^{-2}μmol.m^{-2}.$s^{-1}$$Pa^{-1}$ and similar selectivity was observed.

Meyer, proposed a $CsHSO_4$ impregnated membrane with different supports [53]. Impregnating various membranes, namely, glass fibre, Z450, S450 and ZrO_2 membranes, which were characterized by permeability tested by Gas Chromatography. The permeability test reveals that Whatmann® glass fibre membrane impregnated with $CsHSO_4$ is more hydrogen selective (H_2:CH_4=5 and H_2:CO_2=10) with a H_2 permeance of 1.0 x 10^{-1} – 1.5x 10^{-1} μmol.m^{-2}.$s^{-1}$$Pa^{-1}$, CH_4 permeance of 3.0 x 10^{-2} – 2.5x 10^{-2} μmol.m^{-2}.$s^{-1}$$Pa^{-1}$ and a CO_2 permeance 1.0 x 10^{-2} – 1.5x 10^{-2} μmol.m^{-2}.$s^{-1}$$Pa^{-1}$ as compared to the other membranes and salts with low permeance and selectivity.

$CsHSO_4$/SiO_2 membranes have been identified as a good candidate for gas recovery from UCG syn gases. This is due to the low temperature syngas formed and the need to produce a membrane that can operate at low temperatures. Pd membrane is a good candidate to separate H_2 from syngas but its major limitation is its operation temperature,

2.2.4 Summary of literature review:

Based on the literature review it was shown that dense Pd alloy membranes are good candidates for H_2 separation, showing high permeability and selectivity. The only limitation that hinders the efficiency of the membrane is membrane embrittlement that induces membrane degradation. Organic membranes are also good candidates but are limited to their thermal and chemical stability. From the previous work undertaken in the Honours thesis [52] and work done by Bladergroen et al [1], $CsHSO_4/SiO_2$ composite membrane were identified as good candidates for low temperature separation.

Impregnation, drying and pressing are the membrane preparation technique utilized. The preparation procedure is remarkable simple, fast and cost effective compared all other membrane production techniques.

3 EXPERIMENTAL:

This section is subdivided into the following five parts:

- The preparation of the salt component (section 3.1),
- Membrane preparation (section 3.2),
- Stability and reproducibility of optimized membrane (section 3.3)
- Identification of the transport mechanism (section 3.4) and
- Characterize procedures (section 3.5),

The various steps of the membrane preparation procedure have been optimised to prepare the most effective membrane in terms of permeance and Idea selectivity (3.2). After the optimal salt component, impregnation, drying and pressing procedure had been formulated the stability and reproducibility of the membrane was tested (section 3.3) an finally an attempt was made to investigate the transport mechanism of the H_2 through the $CsHSO_4$ membrane (section 3.4). All standard characterization methods and procedures used in this work are discussed in this section 3.5.

3.1 PREPARATION OF THE SALT COMPONENT OF THE MEMBRANES:

Two different salt components were used to prepare all the membranes discussed in this study. The preparation of the salts, $CsHSO_4$ and $NaHSO_4$, are discussed below in section 3.3.1 and 3.3.2 respectively.

3.1.1 Preparation of $CsHSO_4$:

17.65g of Cs_2CO_3 (Sigma Aldrich 99%) was dissolved in 25ml-distilled water. 10.85g of H_2SO_4 (Kimix 99%) was added to 100ml of distilled water. The Cs_2CO_3 solution was added into the H_2SO_4 solution with a pasteur pipette over a period of time and allowed to stir for 30 min. A saturated $CsHSO_4$ solution was obtained by evaporation of the water at 110°C under constant stirring until crystals were visible at the bottom of the glass beaker. In order to analyse the salt, the saturated solution was dried at 110°C in an oven for 8 hours. The dry salt was analysed further IR to confirm its identity

3.1.2 Preparation of $NaHSO_4$:

5.74 g of Na_2CO_3 (Sigma Aldrich 99%) was dissolved in 25ml distilled water by stirring. 10.85g of H_2SO_4 (Kimix 99%) was added to 100ml distilled water and allowed to stir. The Na_2CO_3 solution was added dropwise to the H_2SO_4 solution with a pasteur pipette over a period of time and stirred for 30 min. A saturated $CsHSO_4$ solution was obtained by evaporate of the water at 110°C under constant stirring until crystals were visible at the bottom of the glass beaker. In order to analyse the salt, the saturated solution was dried at 110°C in an oven for 8 hours. The dry salt was analysed further IR to confirm its identity

3.2 MEMBRANES PREPARATION:

This section is subdivided into the three parts:

- Impregnation of the membrane support (section 3.2.1)
- Drying procedure (section 3.2.2)
- Pressing procedure (section 3.2.3)

Unsupported films of $CsHSO_4$ or $NaHSO_4$ show poor mechanical stability, which makes the permeance experiment difficult since cracks will appear when an slight absolute pressure difference is applied over the membrane. As stated by Meyer [53], glass fibre support (Whatmann®) were identified as the best support for preparation of the $CsHSO_4$ composite membranes. The support added sufficient mechanical strength and obtained membranes showed an acceptable film thickness.

3.2.1 Impregnation of the membrane support:

Impregnation of the glass fibre support with saturated salt solution was done by means of a pasteur pipette. The saturated solution was dripped slowly and absorbed into the glass fibre support. The 1ml optimal volume of saturated solution adsorbed into the support, this is discussed in section 4.1.3.

In order to determine the optimal composition of the composite membrane, four different volumes of saturated $CsHSO_4$ solution were impregnated into the support as shown in Table2. In order to verify if other salts would result in selective membranes as well, $NaHSO_4$ was impregnated into the Whatmann support. Details are given in Table 3

The impregnated supports were allowed to dry for 72 hrs at 25ºC followed by 80ºC overnight. The impregnated membrane was then pressed at 200bars and 160ºC for 2 mins (more details are given in section 3.4). These membranes were then subjected to permeance measurement (see section 3.5.1 for details).

Table 3.1: Volume of $CsHSO_4$ solution impregnated into glass fibre support

Sample #	Impregnated volume of saturated $CsHSO_4$ (ml)	Weight percent $CsHSO_4$ (w%)	Comments
FMA	1	100 (PURE)	Cracked surface
FMB	1	91	
FMC	2	95	
FMD	4	99.5	
FMZ	0	0	Support only

Table 3.2 Different salts impregnated into the glass fibre supports

Sample #	Impregnated volume of saturated Salt (ml)	Weight percent $CsHSO_4$ (w%)
FMX	1ml $NaHSO_4$	89%
FMB	1ml $CsHSO_4$	91%

3.2.2 Optimization of the drying procedure:

The glass fibre support was impregnated with 1ml of saturated $CsHSO_4$ solution. The impregnated membrane was first dried for 72 hrs at room temperature and then at different temperatures overnight as shown in Table 4. The impregnated membrane was then pressed at 160ºC and 200bars for 2minutes (more details are given in section 3.4). These membranes were then subjected to permeance measurement (as discussed later).

Table 3.3: Drying temperatures of the impregnated Glass fibre support

Sample #	1st drying stage: Temperature (ºC)	2nd drying stage: Temperature (ºC)
FME	RT	RT
FMF	RT	80
FMB	RT	160

3.2.3 Optimization of the pressing procedure:

The impregnated and dried support (composite) was pressed into thin films using a hot pressing method. The hot press consisted of a 10-ton hydraulic press and two aluminium plates with two build-in 100W heating elements. The temperature of the aluminium blocks was controlled by a J-type thermocouple connected to a Gefran 400 temperature control unit. The impregnated support was placed between two Teflon® sheets and placed between the metal plates. The holder was then placed between the aluminium heating blocks and maintained at 160ºC and then pressed at 200bar for 2min.

Glass fibre supports were impregnated with 1ml of saturated $CsHSO_4$ solution (according to section 3.2), and dried at 25ºC for 72h, followed by drying at 80ºC overnight. These impregnated supports were pressed at different temperature and pressures as shown in Table 5. These prepared membranes were then subjected to permeance measurement (as discussed in section 3.5.1)

Table 3.4: Whatmann Impregnated membrane pressed at different pressures and temperatures.

MEMBRANE	***PRESSING***	***TEMP***
FMG	0	25
FMH	400	160
FMB	200	160
FMI	100	160
FMJ	200	100
FMK	200	40

3.3 STABILITY AND REPRODUCIBILITY OF OPTIMIZED MEMBRANES:

This section presents an investigation of the consistency of the optimized membrane preparation method. The reproducibility of the membrane properties are discussed (see section 3.3.1) together with results on the stability of the membrane during permeance experiments (see section 3.3.2).

3.3.1 Reproducibility of the membrane properties

In order to investigate the reproducibility of the membrane preparation procedure, 10 membranes were prepared according to the optimized preparation conditions. These conditions were:

- 1ml saturated $CsHSO_4$ solution impregnated in to glass fibre support
- Drying of the impregnated support at 25ºC for 72hrs
- 2^{nd} drying stage at 80ºC overnight
- Pressing the dried impregnated support at 160ºC and 200bar.

Permeance of H_2, CH_4 and CO_2 were sequentially measured for all membranes using the standard procedure, which is discussed in section 3.5.1.

3.3.2 Chemical stability of the membranes

In order to study the stability of the membrane during permeance measurements, the H_2 permeance of FMB1 was measured as a function of time at 25ºC and 140ºC. 50ml of H2 was introduced into the feed side of the membrane reactor (see section 3.5.1.2) over a period of 200min. Gas permeate aliquots were analysed in 10 minute intervals over the 200min period.

3.4 IDENTIFICATION OF TRANSPORT MECHANISM:

In order to find a plausible explanation for the observed Idea selectivity for $CsHSO_4$ membranes a set of characterization experiments were. The characterization involved:

- membrane permeance as function of temperature (section 3.4.1)
- Phases of $CsHSO_4$ (section 3.4.2)
- Proton conductive properties of the $CsHSO_4$ composite membrane (section 3.4.3)

3.4.1 **Membrane permeance as function of the temperature**:

The membrane was subjected to permeance measurement at various temperatures ranging from 25°C - 180°C (Table 6) and the respective selectivities calculated. The membranes were evaluated using H_2, CH_4 and CO_2 gases. Analyte gas was allowed to flow for 30 min before any analysis was performed. The following membranes were analysed:

Table 3.5 Permeance measurements over different temperature ranges.

MEMBRANE	**TEMPERATURE (ºC)**	**H_2**	**CH_4**	**CO_2**
FMB3	25-180	√	√	√
FMB4, 5,6 (1^{ST}, 2^{ND}, 3^{RD})	25-130	√		
FMB7	140-180	√		

Details about the permeance experiment and the equipment are discussed in section 3.5.1

3.4.2 Phases of $CsHSO_4$:

The aim of the experiment was to identify the existence of $CsHSO_4$ and its corresponding phases in the pure synthesised $CsHSO_4$ and in the composite membrane. XRD, TGA and Impedance spectroscopy were used to analyse the various phases of $CsHSO_4$. The preparation of the various samples for each analysis is discussed separately (section 3.4.2.1, 3.4.2.2 and 3.4.2.3 respectively).

3.4.2.1 XRD analysis:

The membranes were analysed by XRD at various stages of the membrane modification and different H_2, CO_2 and CH_4 exposure conditions as shown in Table 7. The optimised membrane was exposed sequentially to H_2 for 1hr followed by CH_4 and CO_2 for 20min each and then analysed. All samples were analyzed using the XRD equipment at the University of Cape Town (UCT). Note that all the experiments were conducted at room temperature. Details about this technique and the equipment that was used is given in section 3.5.3..

Table 3.6: membrane under different conditions

MEMBRANE	**TEMPERATURE**	**EXPOSURE** (to H_2, CH4 and CO_2)
FMA	25	
FME	25	
FMG	25	
FMB	25	
FMB2	25	EXPOSED
FMB3	80	EXPOSED
FMB4	110	EXPOSED
FMB5	130	EXPOSED
FMB6	140	EXPOSED
FMB7	160	EXPOSED

3.4.2.2 Thermal analysis:

The aim of the experiment was to examine the decomposition and the phase changes of the material as a function of time. This was done by weighing 9-10mg of sample and placing it into the sample vial. The following samples were subjected to a heating and cooling cycle between 25ºC – 200ºC, with a flow of air.

- FMA ($CsHSO_4$)
- FMB ($CsHSO_4/SiO_2$)

- FMC (2ml $CsHSO_4/SiO_2$, section 3.2.1, table 2)
- Glass fibre (Whatmann® (SiO_2))

All samples were analyzed using the simultaneous thermal analyzer. Details about this technique and the equipment that was used is given in section 3.5.5

3.4.2.3 Proton conductive properties of the $CsHSO_4$ composite membrane:

The aim of the experiment was to determine the proton conductive properties of the $CsHSO_4$ powder and membranes.

The following membranes were studied after heating and cooling from 25ºC-200ºC:

- Commercial glass fibre support.
- $CsHSO_4$ membrane (FMA), which was prepared as described in section 3.1.1.
- FMB, prepared via the optimized membrane preparation conditions (section 3.3.1)
- FMC (2ml $CsHSO_4/SiO_2$, section 3.2.1, table 2)
-

The proton conductivity of the samples was analyzed using impedance spectroscopy. The analytical procedures of this technique are described in section 3.5.4

3.5 GENERAL CHARACTERIZATION:

This section discusses the means through which the characterization was dealt with, i.e background information, reactor design and sample preparation of the characterization techniques. Section 3.5.1 deals with the permeance measurements, section 3.5.2, with IR, followed by section 3.5.3 with XRD , section 3.5.4 with impedance and section 3.5.5 with TGA.

3.5.1 Permeance measurements:

3.5.1.1 Sample preparation

The assayed membrane was supported on a flat aluminium ring. This 99% aluminium plate has an OD = 50mm, ID = 15mm and a thickness of 15mm. The gasket maker (100% Silicon rubber-Black R.T.V) was used to adhere and seal the membrane onto the aluminium plate. Black R.T.V gasket maker was used because it can operate at temperatures from of 62 – 280ºC. 1mm thick Black R.T.V gasket maker was placed on the aluminium ring, followed by the membrane as illustrated in Fig. 1. This was allowed to dry for 24 hrs.

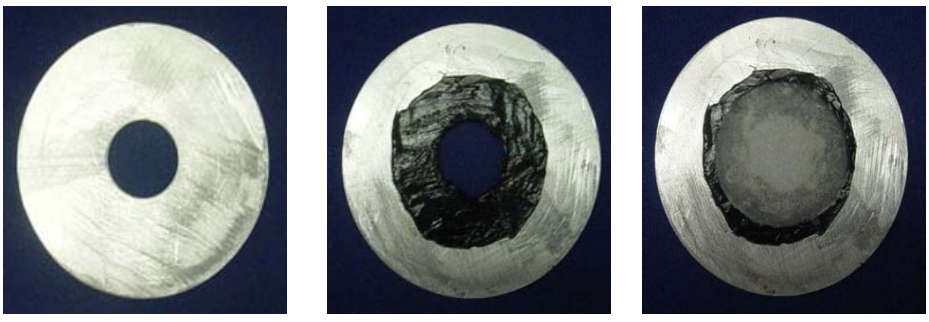

Fig. 1: Prepared membrane adhered on a support

3.5.1.2 Experimental setup:

The permeance measurements were executed using the setup illustrated in Fig.2

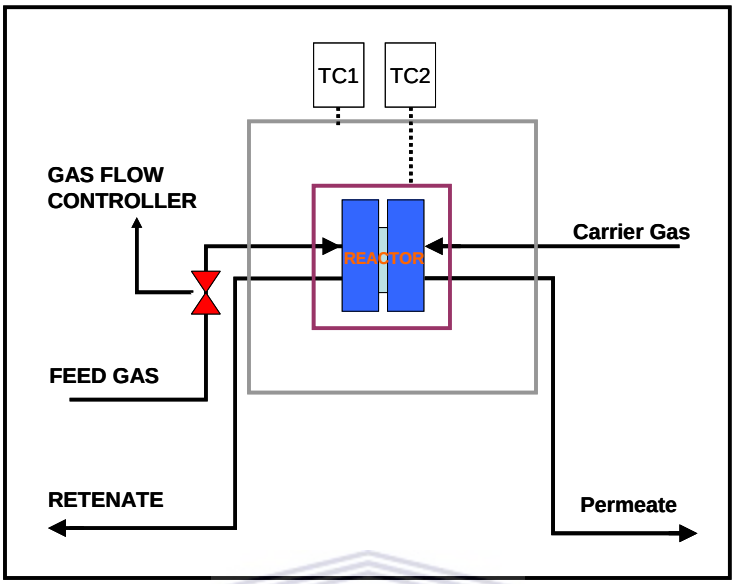

Fig. 2: Schematic gas permeation unit for single gas permeance measurements.

The system is comprised of four units that operate in unison, to accurately measure the permeance and consequently generate the Idea selectivity by calculation. The four operating units in the permeance measurement are: 1) a Reactor illustrated in Fig 3. 2) the heat contributor which is supplied by a conventional oven,3) gas lines, which handle feed gas, retentate, sweep gas and permeate and 4) the gas chromatograph, which is used to analyze the concentration of the permeates. Details about item 1-4 will be discussed separately below.

Reactor

The reactor, illustrated in Fig 3, is a flat membrane reactor. The reactor is perceived as the heart of the experiment because it acts as a holder for the assayed membrane. The reactor was carefully designed in order to facilitate sequential permeance measurements of various gases (H_2, CH_4 and CO_2), with sufficient control and no gas leaks. The reactor was constructed from stainless steel to accommodate the high temperature and prevent rust.

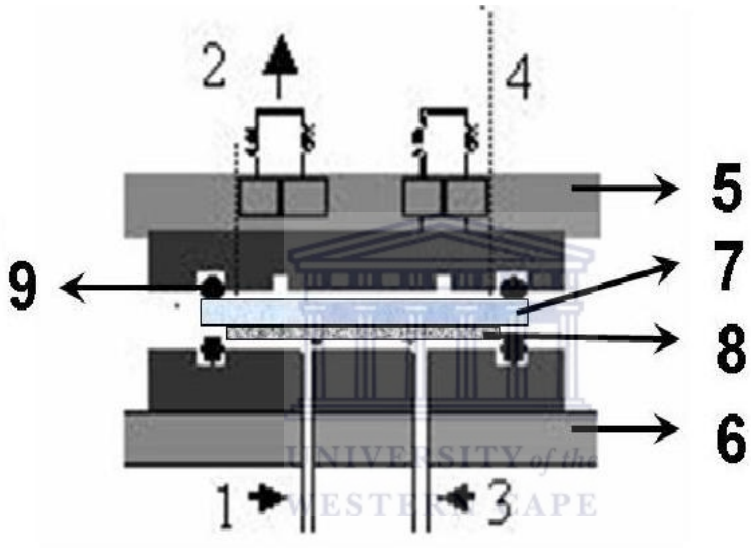

Fig. 3: Schematic representation of the Reactor:(1) feed, 2) permeate, 3) reject, 4) inlet for Sweep gas, 5) permeate steel base, 6) feed steel base, 7) sintered Metal support 8) membrane, 9) O-ring).

The reactor comprises from two sections, the feed side and the permeate side. Both the feed and permeate sides contains O-rings that were embedded into the rear of the bases. These O-rings are essential to reduce gas leaks. The reactor was fixed with Viton O-rings,

which had an ID = 45mm, OD= 48mm and a thickness of 1.5mm. Viton O-rings consist of inorganic material, which can operate at temperatures in the region of 25- 220ºC. The feed side of the reactor was fitted with Swagelok® unions as an outlet and an inlet for gas feed and retentate respectively. The base also contained a recess of 20mm to allow flow from the inlet to outlet on the feed side. The permeate side of the reactor was also fitted with Swagelok® unions as an outlet and an inlet for permeate and N_2 carrier gas respectively. Four 10cm bolts and wing nuts held these two sections together.

The supported membrane was then insert into the Reactor and aligned to obtain a leak-free system.

Convection oven

The reactor was placed into the convection oven and connected to the gas lines. The convection oven can operate at temperatures from 25ºC to 220ºC. It is equipped with Thermal couples T1 and T2, where T1 is used to detect the temperature of the reactor and T2, used with a digital display, to detect the temperature of the convection oven and to regulate the temperature.

Analyte gases

The gases (H_2, CH_4 and CO_2) were supplied from gas cylinders at a pressure of 400kPa via ¼" Swagelok® tubing. The end of the gas lines was fixed with a ¼" ferrule and nut which

was connected via ¼'' Swagelok® male union to the reactor and the gas cylinders. The gas supply was fed into the reactor, from the feed inlet (1). Gas lines from the H_2, CH_4, CO_2 gas cylinder, converged into a single gas line which was connected to the reactor via the permeate inlet. Swagelok® valves controlled all the gas lines and the single gas line.

The membrane was tested sequentially, with a single gas permeance measurement with H_2, CH_4 and CO_2. The gas under investigation was allowed to flow at a constant rate of 50ml/min through a gas flow meter at 1 atmosphere pressure gradient. Permeance measurements of the gases under investigation were conducted via Gas Chromatography**.**

Gas Chromatography:

The permeance measurement was investigated via a Gas Chromatography (GC) (GowMac). The instrument operates at a current of 70mA, a column temperature of 30ºC and an injection port temperature of 40ºC.

The column utilized was a 6ft stainless steel Porapak Q column, with a inner diameter of 2.2mm and a outer diameter of 3.2mm. The Porapak Q column can operate at a maximum temperature of 230ºC and have a mesh length of 100/120.The column operates with ultra high purity N_2 (99.999%) gas at a carrier gas at constant flow rate of 0.5ml/sec.

The GC was connected to a computer, which hosted the Borwin® software utilised to quantify the results. The Gas Chromatography system was initially calibrated by adjusting the N_2 carrier base gas to zero. The system is then ready to operate.

3.5.2 Infra red:

In principle, Infrared spectroscopy works because chemical bonds have specific frequencies at which they vibrate corresponding to natural energy levels. It is a technique that involves the absorption of electromagnetic radiation in the infrared region of the spectrum, which results changes in the vibrational energy of molecule. Since all molecules resonate in the form of stretching, bending, etc., the absorbed energy will be utilized in changing the energy levels associated with these. It is a valuable and formidable tool in identifying compounds [40].

INSTRUMENTATION:

Basically it is a double beam spectrophotometer comprising IR source (usually a red hot ceramic material), grating monochromator, thermocouple detector, cells made of either sodium chloride or potassium bromide materials, etc. A beam of IR light that was produced and split into two beams, measures the sample energy at different wavelengths. One of the beams is passed through the sample and the other passed through the solvent. The beam is then reflected back towards a detector, but before it reaches the detector, they first pass through a monochromator. Before running the sample you should run the instrument with a reference or a blank. The following is the simplified version of the instrument:

A reference is used for two reasons:

1] This prevents fluctuations in the output of the source affecting the data.

2] This allows the effects of the solvent to be cancelled out within the material.

APPLICATIONS:

It finds extensive use in the identification and structural analysis of organic compounds, natural products, polymers, etc [40]. The presence of particular functional group in a given organic compound can be identified. Since, each and every functional group has its own vibrational energy, the IR spectra can be seen as their fingerprints. This technique will be used in the following research to analyse inorganic $CsHSO_4$ and $NaHSO_4$ and its relevant SiO_2 membranes. Identifying the wavelengths of HSO_4 within the investigated material would clarify the presence of $CsHSO_4$ and $NaHSO_4$ and its relevant SiO_2 membranes

SAMPLE PREPARATION:

IR samples were prepared by mixing and pressing 10mg synthesized salt and 990mg of CsI. The window used in this case was KBr or CsI. The samples were then prepared by pressing the mixture to form a pellet, which was done at 10 tons for 5 min.

3.5.3 X-ray diffraction:

X-ray diffraction crystallography is a technique in which the pattern produced by the diffraction of X-rays through the closely spaced lattice of atoms in a crystal is recorded and then analyzed to reveal the nature of that lattice [41]. The spacing in the crystal lattice can be determined using Bragg's law.

PRINCIPLE:

During analysis, when the X-ray penetrates the atoms, it induces an electromagnetic wave motion of the electronic cloud [41]. The movement of these charges re-radiate waves with the same frequency, which in known as Rayleigh scattering as shown in Fig. 4.

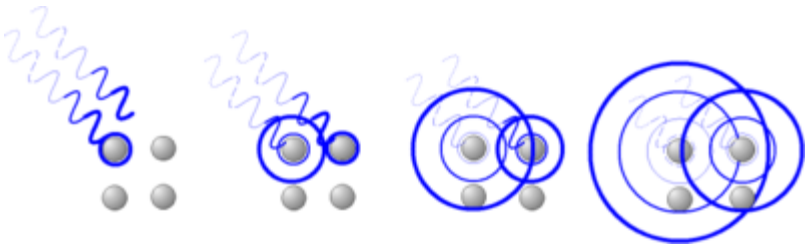

Fig. 4: The X-ray penetration inducing Rayleigh scattering

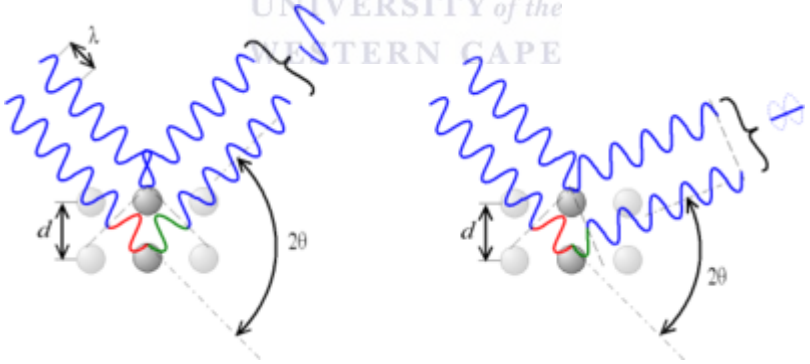

Fig. 5:According to the 2θ deviation, the phase shift causes constructive (left figure) or destructive (right figure) interference.

The re- emitted X-ray interference, gives rise to constructive and destructive interference as shown in Fig. 5, this is known as the diffraction phenomenon. Constructive

interference is induced when the phase shift is proportional to 2θ, which can be expressed by Bragg's law.

$$n\lambda = 2d\sin(\theta)$$

.

where

n: is the order of diffraction, and is an integer (n =1, 2, 3, etc)

λ: is the wavelength of the X-ray , and moving electrons, protons and neutrons.

d: is the spacing between the planes in the atomic lattice

θ: is the angle between the incident ray and the scattering planes.

Note that moving particles, including electrons, protons and neutrons, have an associated wavelength, as determined by Louis de Broglie (see De Broglie wavelength [42])

APPLICATION:

This technique is widely used in chemistry and biochemistry to determine the structures of an immense variety of molecules, including inorganic compounds, DNA and proteins. X-ray diffraction is commonly carried out using single crystals of a material, but if these are not available, microcrystalline powdered samples may also be used, although this requires different equipment, gives less information, and is much less straightforward. In the following research, XRD willed be used to identification the phases of the material under investigation. In this case phase III, II and I of $CsHSO_4$ will be particularly identified.

INSTRUMENT:

It consists of X-ray tube for the source, monochromator and a rotating detector.

The machine used was a Panalytical, PW 3830 X-ray generator that operates at the following settings: voltage of 40Kv, current of 25mA. The analysis was carried out with a α-Cu tube (wavelength = 1.54Å) operating at a scan rate of 0.002º/s, angular resolution of 0.006º, angular degree of 24-32º and time per step of 10 sec. A 1.5cm x 2.5cm rectangle of the membrane was cut out and adhered to the glass support holder.

3.5.4 Impedance

Impedance spectroscopy is a powerful technique for the study of these materials, because it enables the bulk ionic conductivity to be resolved from other resistive or capacitive elements within these conductors [42]. A single crystal ionic sample would show a semicircle in an impedance plot (see Fig. 6), resulting from the bulk resistance and the bulk capacitance of the crystal.

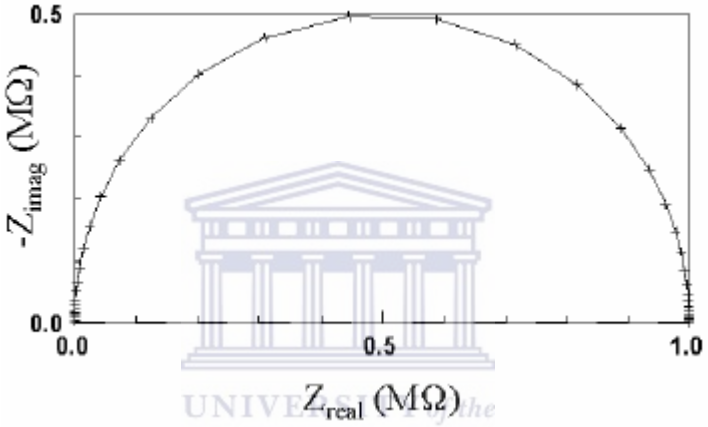

Fig. 6 Cole plot (Z' va Z)

Many of these fast-ionic compounds undergo several phase transitions as they are heated [43]. These transitions would cause single crystals to split up, so they are not commonly used for these measurements. A sintered powder pellet consisting of fine grains of the sample is connected via electrodes or unreactive metal (e.g. silver or platinum) electrodes to an impedance analyser. Impedance spectroscopy provides information about some or all of the following properties: ionic conduction, grain boundary impedance, and electrode/electrode interface characteristics and also mixed conducting solid material

REACTOR SETUP:

The impedance spectroscopy system consists of a furnace, measuring cell and an Autolab PGSTAT30 Impedance Analyser with two electrical measuring points and a dummy cell. The furnace is used to measure impedance at different temperatures. It is made of steel that is insulated with ceramic stone. The temperature control unit was used to monitor the temperature. A homemade measuring cell is shown in Fig 7. It is a 10cm diameter stainless steel tubular cell that has a spring at the base of the measuring cell and maintains a constant pressure on the sample.

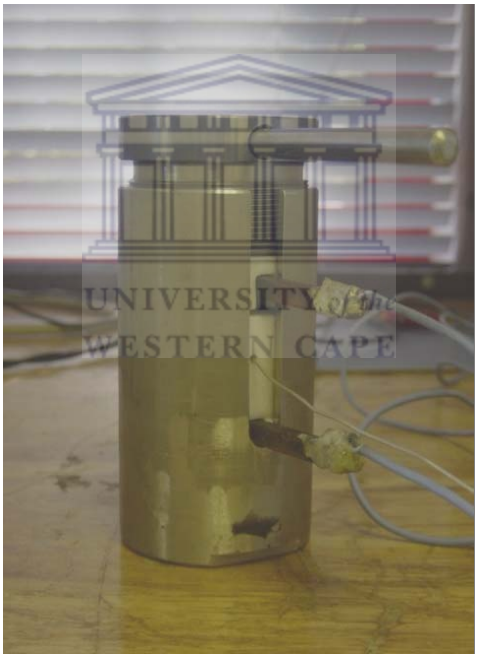

Fig. 7: Homemade measuring cell.

A tubular Teflon® holder set up was placed on the spring and acted as a holder for the first copper electrode. On this copper electrode a stainless steel pistons was placed which made contact to the other stainless steel piston on the topside. Fig. 8, illustrates, the Teflon® holder, the electrode and the pistons, where the Teflon® ring surrounded the

pistons. The cell was closed and pressure was put on the pistons by screwing the iron cover from the top of the stainless steel cylinder. The temperature of the cell was measured by inserting a temperature probe into the measuring cell with caution to prevent short circuits.

Fig. 8 Insulted electrode system

IMPEDANCE ANALYSER

The Impedance analyser or Frequency Response Analyser (FRA) measures the impedance over a frequency range of 10MHz to 32MHz, via measurement integration of the analyser input, for harmonic noise rejection. The Impedance analyser is connected to a P.C, which is loaded with the Frequency Response Analyser (FRA) software, which is used to analyse the results and convert that into a Resistance analogy.

3.5.5 Thermal analysis:

The technique of thermal analysis actually comprises of a series of methods, which detect changes occurring in the physical and mechanical properties of the given substance by the application of heat or thermal energy [46]. The physical properties include mass, temperature, enthalpy, dimension, dynamic characteristics and others. In other words it detects the dependency of physical properties with the temperature and tells the condition of the substances.

The following are the popular methods under this technique:

THERMOGRAVIMETRIC ANALYSIS (TGA):

Simply it is also called as thermogravimetry (TG). Here the change in sample weight is measured while the sample is heated or cooled at a constant rate. This technique is effective for quantitative analysis of thermal reactions that are accompanied by mass changes, such as evaporation, decomposition, gas absorption, desorption and dehydration.

DIFFERENTIAL SCANNING CALORIEMETER (DSC):

This technique measures the amount of heat absorbed or released by a sample as it is heated or cooled or kept at constant temperature (isothermal) [47]. In actual practice the sample and reference material are simultaneously heated or cooled at a constant rate. The difference in temperature between them is proportional to the difference in heat flow (from the heating source i.e. furnace), between the two materials. It is the well-suited technique in the detection and further studies of liquid crystals. This technique is applied

to most of the polymers in evaluating the curing process of the thermoset materials as well as in determining the heat of melting and melting point of thermoplastic polymers. Through the addition process of isothermal crystallization it provides information regarding the molecular weight and structural differences between very similar materials [61].

INSTRUMENATION:

The micro-balance plays a significant role here. During the process of measurement, the change in sample mass affects the equilibrium of the balance. This imbalance is fed back to a force coil, which generates additional electromagnetic force to recover equilibrium. The amount of additional electromagnetic force is proportional to the mass change. During the heating process the temperature may go as high as 10000 C inside the furnace.

APPLICATION:

It finds its application in finding the purity, integrity, crystallinity and thermal stability of the chemical substances under study. Sometimes it is used in the determination of the composition of complex mixtures. This technique has been adopted as testing standard in quality control in the production field, process control and material inspection. It is applied in wide fields, including, polymer, glass, ceramics, metals, explosives, semiconductors, medicines and foods [46]

TGA and DSC will be utilized in this case to identify the stability, phase transition of $CsHSO_4$ and relevant SiO_2 membranes as a function of temperature.

SAMPLE PREPARATION:

The membrane material was cut into smaller pieces. 9-10mg of the sample (membrane or powder) was weighed out and placed in the TGA crucible. The analysis was performed in H_2 or air over a temperature range from thermal cycle between 25ºC-200ºC at a scan rate of 5ml/min under air.

4 RESULTS AND DISCUSSION:

4.1 PREPARATION OF THE SALT COMPONENT OF THE MEMBRANE:

Two salts were prepared as the main components for the membranes discussed in this study. $CsHSO_4$ and $NaHSO_4$ are described in section 3.1. The $CsHSO_4$ salt is not commercially available. The Infra-red (IR) spectroscopic characterization of both salts will be discussed separately.

4.1.1 $CsHSO_4$ salt

The synthesis of $CsHSO_4$ was done by simple wet chemistry as described in section 3.1.1. Upon the addition of Cs_2CO_3 solution to the H_2SO_4 solution, gas bubbles evolved from the mixture, which was expected to be CO_2.

$$Cs_2CO_3 + 2H^+ + 2HSO_4^{--} \rightarrow 2CsHSO_4 + CO_2\,(g) + H_2O \qquad [1]$$

$$Cs_2SO_4 + H_2SO_4 \rightarrow 2CsHSO_4 \qquad [2]$$

The crystals obtained from the prepared solution were analyzed by Infra-red (IR) spectroscopy. For reference purposes, Cs_2CO_3 (Kimix 99.0%) and Cs_2SO_4 (Alfa Aesar, 99.5%) was analyzed by IR. The IR spectra of all three samples are shown in Fig. 9. In the IR spectrum of sample 1, bands are observed at 850, 1000 and 1250cm^{-1}, suggesting the presence of HSO_4. The presence of S-O is also evident, due to a band at 1125cm^{-1}. The spectrum also suggested the presence of OH, which is due to absorption bands at

560cm^{-1}, 3200 cm^{-1}, 1650cm^{-1} and 2900cm^{-1}, most likely in the form of crystal water. The IR spectrum of Cs_2CO_3, clearly shows a broad band in the range of 1450cm^{-1} which reflects the C-O bond and a sharp band at 2900cm^{-1}, which is due to O-H. The IR spectrum of Cs_2SO_4, showed a sharp and a broad band in the range of 1130cm^{-1} and 580cm^{-1} respectively, which is due to S-O bonding.

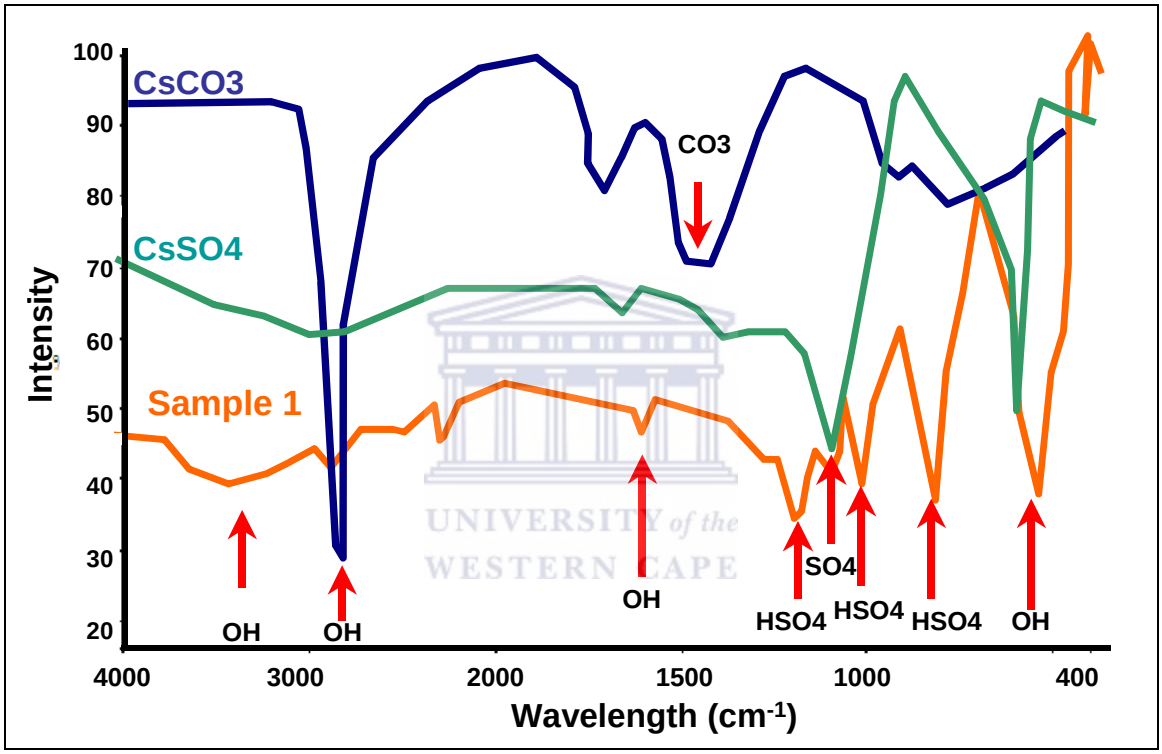

Fig. 9: IR spectrum of the, (a) synthesis product (sample 1), (b) Cs_2CO_3 and (c) Cs_2SO_4

Comparison of the spectra (Cs_2SO_4, Cs_2CO_3 and sample 1) leads to the conclusion that sample 1 consists mainly of $CsHSO_4$. The absence of the C-O band indicates the complete conversion of the starting material (Cs_2CO_3).

4.1.1.1 IR sample preparation: KBr vs CsI

The IR spectra given in

Fig. 10 show why the IR samples of $CsHSO_4$ should be prepared with CsI and not with KBr.

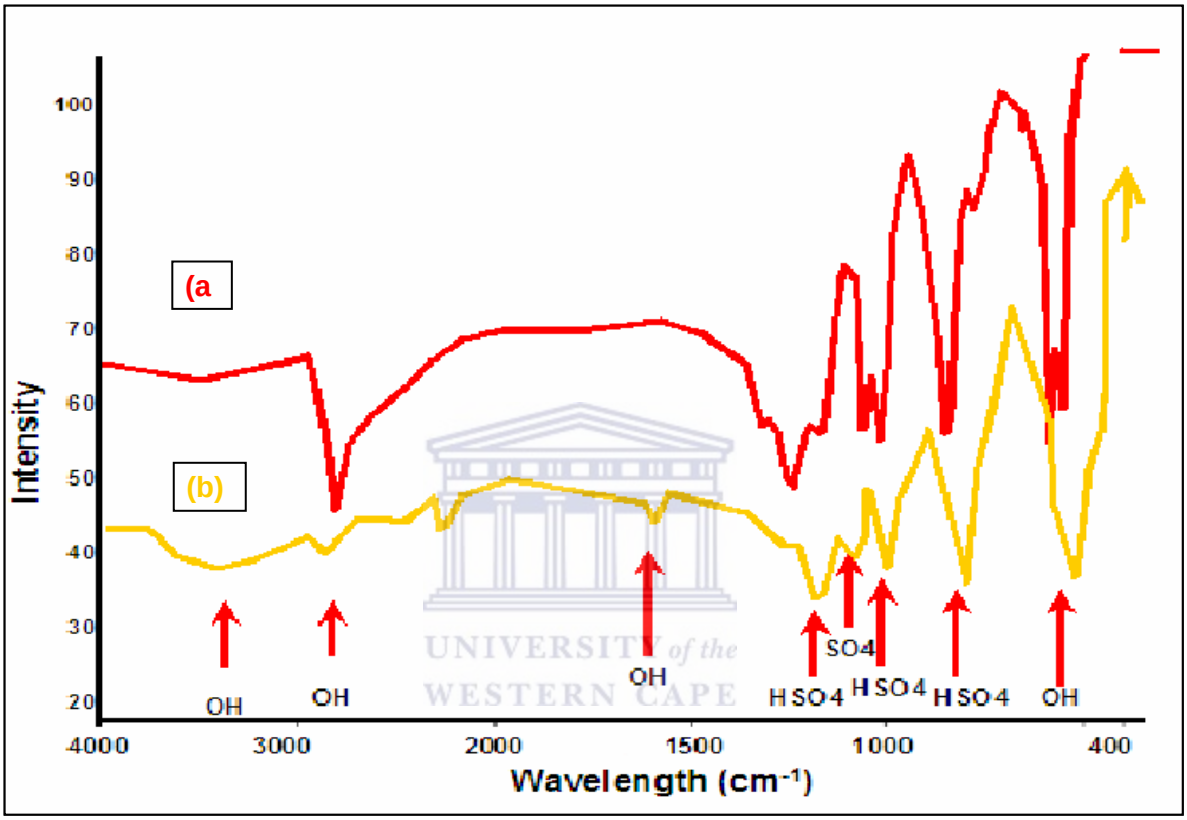

Fig. 10: IR spectrum of (a) $CsHSO_4$ with KBr and (b) $CsHSO_4$ with CsI.

The IR sample prepared by mixing $CsHSO_4$ with KBr shows bands that are evident for HSO_4 at 850, 1000, 1250cm^{-1} and some bands for SO_4 and OH group. But a distinct band at 1064cm^{-1} is evident in the spectrum. Accordance to Baran *et al,* the presence of the band at 1064cm^{-1}, suggests the presence of $KHSO_4$ and not $CsHSO_4$ [28]. The existence of $KHSO_4$ is due to the exchange between Cs^+ and K^+, which is induced by water. In the

latter case, $CsHSO_4$ pressed with CsI (spectrum b) shows a spectrum that proposes the existence of $CsHSO_4$.

4.1.2 $NaHSO_4$ salt:

The synthesis of $NaHSO_4$ was done by simple wet chemistry as described in section 3.1.2. Upon the addition of Na_2CO_3 solution to the H_2SO_4 solution, gas bubbles evolved from the mixture, which was expected to be CO_2.

$$Na_2CO_3 + 2H^+ + 2HSO_4^{--} \rightarrow 2NaHSO_4 + CO_2\,(g) + H_2O \qquad [3]$$

The crystals obtained from the prepared solution were analyzed by Infra-red (IR) spectroscopy. The IR spectrum of sample 2 is shown in Fig. 11. For reference purposes, the IR spectrum of $CsHSO_4$ is added as well.

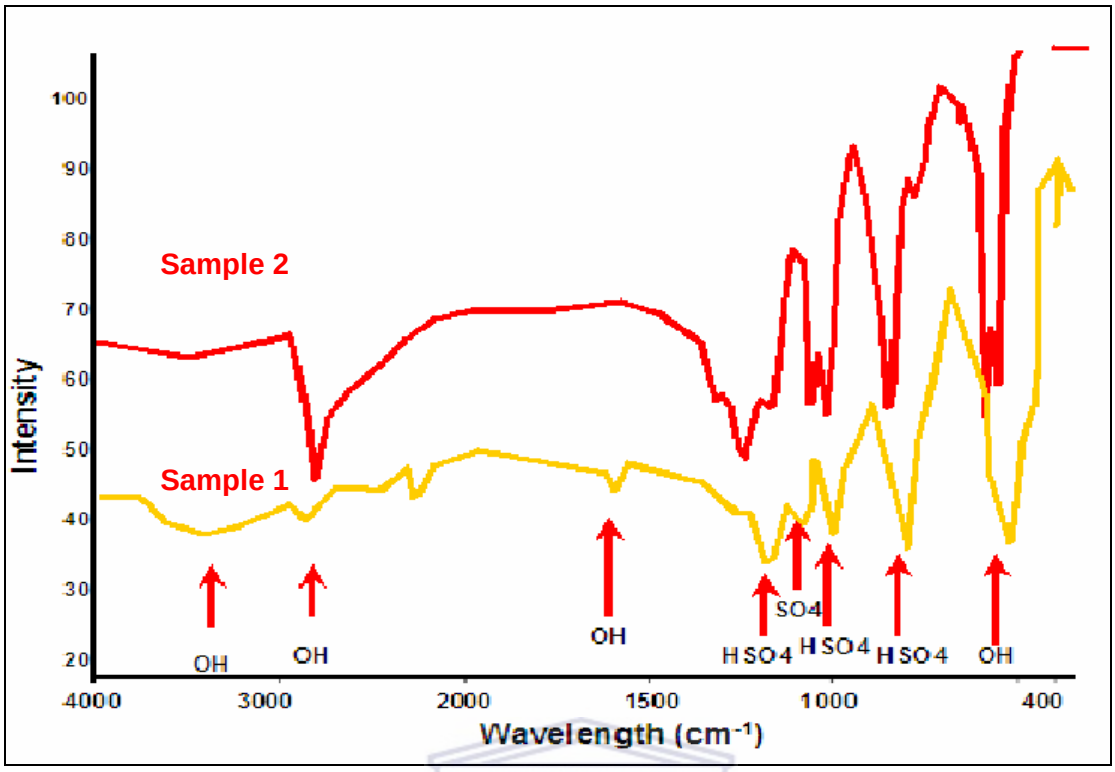

Fig. 11: IR spectrum of $NaHSO_4$ and $CsHSO_4$.

The existence of HSO_4 is evident due to the presence of absorption bands at 850, 1000 and 1250cm^{-1}. By comparing the two spectra, an additional band at 1064cm^{-1} is observed. This is due to the $NaHSO_4$ material. The presence of S-O is also apparent, due to a band at 1125cm^{-1}

Bands in the range of 3100cm^{-1}, 2900cm^{-1}, 1650$cm^{-1}$and 560cm^{-1} are due to the existence of O-H present in the matter, with a more prominent band at 2900cm^{-1} compared to $CsHSO_4$. This is due to the hydrophilic nature of $NaHSO_4$. The spectrum in Fig. 3 suggests that $NaHSO_4$ was successfully prepared.

4.2 MEMBRANE PREPARATION:

The need to develop a reproducible preparation method for a defect free H_2 selective membrane that is industrially accepted is great. This was done by optimising the composition, drying temperature and pressing conditions. All these individual preparation steps are discussed below.

As will be shown in the section below the optimized membrane preparation method is as follows:

- Impregnation procedure; 1ml saturated $CsHSO_4$ solution per glass fibre support
- drying procedure; 3 days at 25ºC followed by 12 hours at 80ºC
- pressing procedure; 2min pressing at 150ºC and 200bars.

4.2.1 Impregnation of the membrane support:

The sample composition of $CsHSO_4/SiO_2$ prepared is illustrated in Table 4.1. The $CsHSO_4$ percentage is relative to the weighted membrane. Sample FMX was prepared by impregnation of the glass fibre support with 1ml saturated $NaHSO_4$ instead of $CsHSO_4$

Table 4.1: Permeance measurements of different weight percent of $CsHSO_4$

Sample	Weight percent	Permeance ($\mu mol \cdot m^{-2} \cdot s^{-1} \cdot Pa^{-1}$)			Idea selectivity	
#	$CsHSO_4$ (w%)	H_2	CH_4	CO_2	H_2:CH_4	H_2:CO_2
FMZ	0 (x=1)	1.5	1.3	1.1	1	1
FMB	91 (x=0.9)	0.156	0.0273	0.01	6	10
FMC	95 (x=0.05)	0.072	0.014	0.008	5	9
FMD	99.5 (x=0.005)	0.010	0.0019	0.0011	5	9
FMA	100 (x=0) (PURE)	Not mechanically stable, no measurement performed				

From the permeance result of the different $CsHSO_4$ to SiO_2 compositions, it is observed that the pure $CsHSO_4$ (FMA) and SiO_2 (FMZ) membrane are not good candidates. Pure $CsHSO_4$ membranes are not capable of being tested due to its fragile nature. SiO_2 shows high permeance and below Knudsen selectivity. However with the combination of the $CsHSO_4$ and glass fibre (SiO_2) material, mechanical strength and significant Idea selectivity is achieved. The composite membrane shows a decrease in H_2 permeance with an increasing of the $CsHSO_4$ content. This is possible due to the increase in thickness, herewith increasing the resistance of the membrane towards the permeating gases. The idea selectivity on the other hand remains almost constant with increasing $CsHSO_4$ content. At 91% composite $CsHSO_4$, the idea selectivity for the H_2:CO_2 and H_2:CH_4 is the highest at 10 and 5 respectively

The conclusion of this section is that the glass fibre supports impregnated with 1ml saturated $CsHSO_4$ solution leads to the composite film with the optimal idea selectivity and 5 and 10 for H_2:CO_2 and H_2:CH_4 and permeance.

Table 4.2 shows the permeance results of only two membranes. Sample FMX that was prepared by impregnation of the glass fibre support with 1ml saturated $NaHSO_4$. Sample FMB, with 1ml saturated $CsHSO_4$ solution. From the results it is shown that the idea selectivity of $NaHSO_4/SiO_2$ remains below the Knudsen value.

Table 4.2: Permeance measurements of $CsHSO_4$ and $NaHSO_4$ membranes

Sample	Weight percent	Permeance ($\mu mol \cdot m^{-2} \cdot s^{-1} \cdot Pa^{-1}$)			Idea selectivity	
#		H_2	CH_4	CO_2	H_2:CH_4	H_2:CO_2
FMB	91 (x=0.9) $CsHSO_4$	0.156	0.0273	0.01	6	10
FMX	91 (x=0.9) $NaHSO_4$	0.251	0.1210	0.08	2	3

4.2.2 Drying Optimisation:

In order to precipitate the $CsHSO_4$ within the fibres of the support, the impregnated support has to be dried. Three membranes were prepared as described in section 3.2.2. Table 4.3 summarized the permeance results of these membranes. The results show that the initial drying temperature is of crucial importance on the H_2 permeance. The result suggests that the impregnated supports need to be dried at 80ºC or higher. The

selectivities of sample FME indicate the presence of large defects. These large defects could have been formed during the pressing procedure at 160°C, when excessive crystal water is turned into steam and ruptures the membrane film.

Table 4.3 Permeance measurements of $CsHSO_4$ membranes with respect to drying temperature.

Sample	2nd drying stage	Permeance (μmol·m^{-2}·s^{-1}·Pa^{-1})			Idea selectivity	
#	Temperature (ºC)	H_2	CH_4	CO_2	H_2:CH_4	H_2:CO_2
FME	RT	0.690	0.160	0.150	2	2
FMF	80	0.156	0.0273	0.015	6	10
FMB	160	0.140	0.022	0.011	5	9

With the impregnated support dried at 80°C (see sample FMF), a successful membrane was formed which showed selectivities above the theoretical Knudsen values. The properties of membranes dried at temperatures above 80°C did not show any further improvements. In fact the idea selectivity was slightly lower. From this set of experiments it can be concluded that a minimum drying temperature of 80°C is required for the formation of a membrane with decent idea selectivity

4.2.3 Optimisation of the pressing procedure

The pressing procedure is needed for the formation of a continuous film of the $CsHSO_4$. In order to find the optimal pressing conditions, a set of experiments was performed as described in section 3.2.3. The modified support was pressed into a membrane at different pressures (see section 4.2.3.1) and temperatures (see section 4.2.3.2).

4.2.3.1 Optimal pressure

The pressing conditions and permeance results of 4 different membranes are presented in Table 4.4. The impregnated support that is not subjected to the pressing procedure (FMG) does not show any significant idea selectivity. This result could be expected from a support that is only impregnated with a salt. It seems that a continuous film, which is necessary to obtain any gas-selective properties, can only be formed after a significant pressure has been applied on the impregnated support. The three samples that were pressed at 100, 200 and 400bar respectively show selectivities above the Knudsen value. It was observed that the gas permeance decreases with increasing pressure applied over the membrane. This is possibly due to the densification of the membrane. Membranes pressed at 200bars show the best idea selectivity. Pressures above 200bar are expected to make even denser and thinner membranes but no further increase in idea selectivity and a decrease of the gas permeance was observed (FMJ). Membranes produced at 200bar show optimal idea selectivity.

Table 4.4: Permeance results of membranes pressed at various pressures

Sample	Pressure	Permeance (μmol·m^{-2}·s^{-1}·Pa^{-1})			Idea selectivity	
#	(bar)	H_2	CH_4	CO_2	H_2:CH_4	H_2:CO_2
FMG	0	0.9	0.5	0.4	2	2
FMI	100	0.21	0.04	0.025	5	8
FMB	200	0.156	0.0273	0.015	6	10
FMH	400	0.08	0.014	0.009	6	10

4.2.3.2 Optimal pressing temperature

Table 4.5 shows the permeability results of the 4 membranes that are pressed at 200 bar but at different temperatures. From the results it was observed that the permeance of all gasses was decreasing with increasing pressing temperature. The idea selectivity of 3 was observed for both H_2:CO_2 and H_2:CH_4 at 25ºC. While the idea selectivity of H_2:CH_4 seems to be more or less stable at 6 with increasing pressing temperature, the idea selectivity of H_2:CO_2 is increasing. The reasons for the different trends cannot be explained at this point in time. 160°C was selected as the optimal pressing temperature since it resulted in the membrane with the highest overall selectivity.

Table 4.5: Permeance measurements of $CsHSO_4$ membranes with respect to pressing temperature.

Sample	Temperature	Permeance ($\mu mol \cdot m^{-2} \cdot s^{-1} \cdot Pa^{-1}$)			Idea selectivity	
#	(°C)	H_2	CH_4	CO_2	H_2:CH_4	H_2:CO_2
FML	25	0.3	0.12	0.1	3	3
FMK	40	0.23	0.04	0.031	6	7
FMJ	100	0.2	0.03	0.025	7	8
FMB	160	0.16	0.0273	0.015	6	10

4.3 Stability and reproducibility of optimized membranes

Section 4.3 presents an investigation of the consistency of the membrane preparation method, used in this study, and the reproducibility of the membrane properties were discussed (see section 4.3.1) together with results on the chemical stability towards the H_2, CH_4 and CO_2 (see section 4.3.2).

4.3.1 Reproducibility of the membrane properties

As discussed in section 3.3.1, permeance measurements were collected for 10 membrane samples, which were prepared according to the optimized membrane preparation procedure. Fig. 12 illustrates that the H_2:CO_2 and H_2:CH_4 selectivities are on average about 10 and 5, respectively. The results also suggest that the membrane preparation procedure is fairly reproducible in terms of idea selectivity. The low idea selectivity of sample 3 is most

likely a result of the presence of defects in the form of cracks or pinholes, which may have been formed due to incorrect handling of the samples. The small variations of the idea selectivity are likely due to analytical error. One membrane exhibited high H_2:CO_2 and H_2:CH_4 selectivities of 16 and 10 respectively. Apart from the possibility of an analytical error, this may be an indication of the maximum idea selectivity attainable with $CsHSO_4$ membranes even with the absence of small defects.

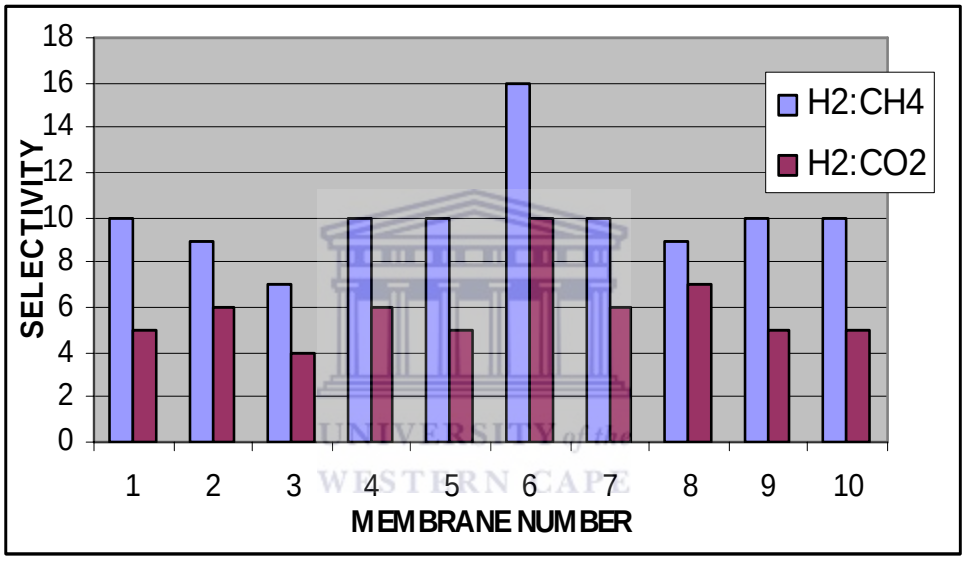

Fig. 12: Idea selectivity data for membranes prepared using the optimized preparation procedure.

4.3.2 Chemical stability of the membranes

In order to continue with meaningful research it was necessary to investigate the chemical stability of $CsHSO_4$ towards the analysis gases. As will be demonstrated in section 4.2, permeance will be measured as function of temperature. The duration of these types of experiments are significantly longer than the "screening" permeance analyses that have been performed up until this point in the study. The effect of time and the exposure of the membrane to the analysis gases were studied in order to ensure that the changes in permeance discussed in section 4.2-4.4 are not a result of chemical instability of the membrane.

The permeance experiment with membrane FM11 is described in detail in section 4.1.1. The results are shown in Fig. 13. The initial H_2 permeance values were reasonably stable as function of time. This indicates that the membrane is not chemically modified (reduced) by H_2. CH_4 does not seem to change any of the membrane's properties since the 2^{nd} H_2 permeance value is the very close to the 1^{st} H_2 permeance value. Exposure of the membrane to CO_2 did also not significantly change the properties of the membrane; the 3^{rd} H_2 permeance measurement was very similar to the 1^{st} and 2^{nd} value.

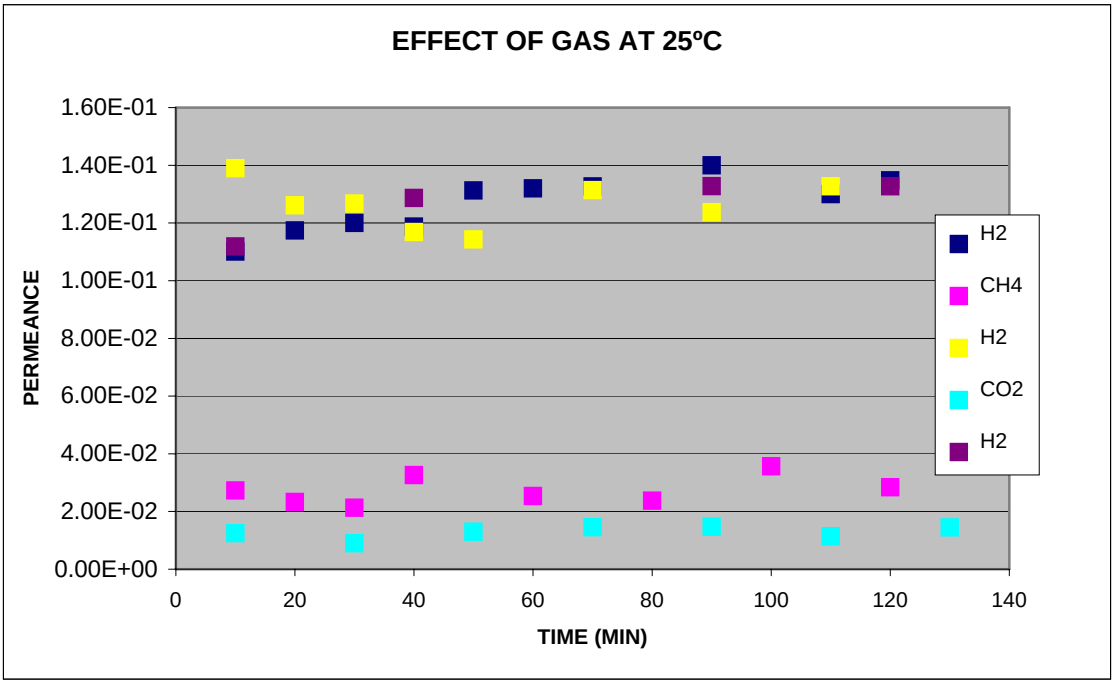

Fig. 13 Gas permeance as a function of time at 25ºC

A similar experiment was repeated at 140°C. The results are depicted in Fig. 14. Again, no significant change of permeance was observed after the membrane was exposed to CH_4 and CO_2. Both experiments indicated that the selective properties of membrane are not affected by exposure of the membrane to CH_4 or CO_2 at temperatures between 24 and 140°C.

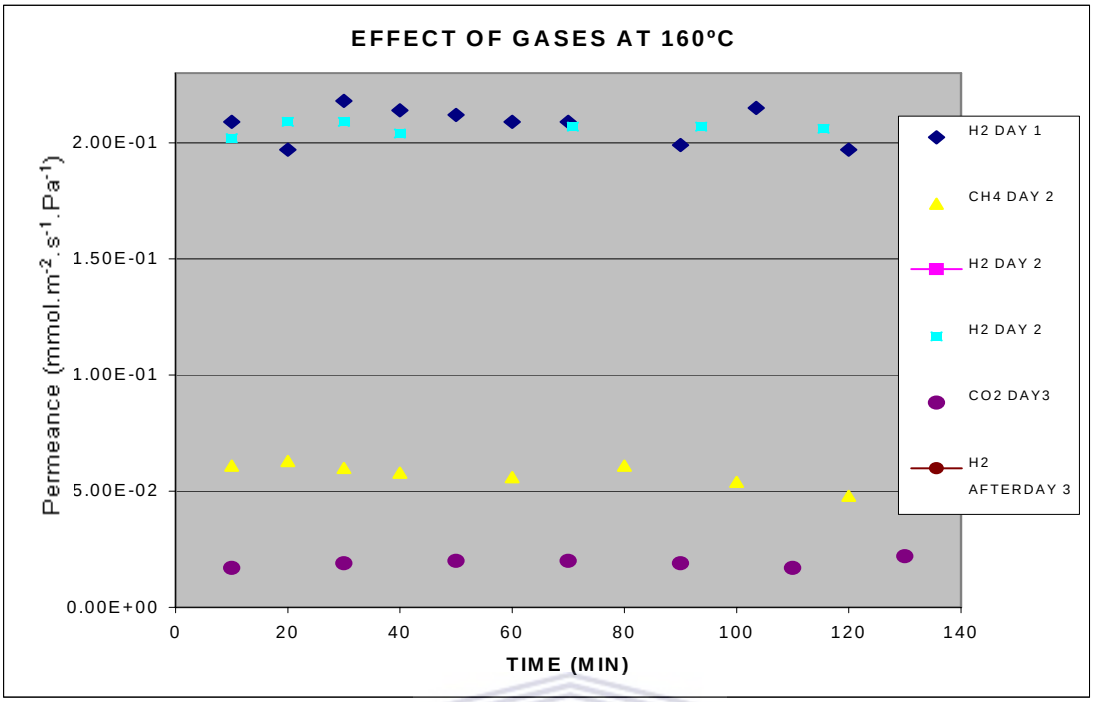

Fig. 14 Gas permeance as a function of time at 140ºC

In section 4.4.2, the XRD of membrane before and after exposure is shown. The XRD pattern confirms that the membrane is not changing upon exposure to analyte gases.

4.4 IDENTIFICATION OF TRANSPORT MECHANISM

The gas selective properties of $CsHSO_4$ membranes have not been reported anywhere before. $CsHSO_4$ was proposed as possible electrolyte for fuel cell applications, (a dense $CsHSO_4$ membrane was used) [64]. In order to explain the unusual selectivities (H_2:CO_2 and H_2:CH_4, 10 and 5 respectively) the gas transport mechanism had to be identified. It is clear that the observed idea selectivity is not just an effect of Knudsen diffusion in a microporous material. The main questions to be answered were:

- How does H_2 transport take place?
- Is hydrogen transported through a solution diffusion mechanism?
- Is molecular sieving possible?
- Is hydrogen transported in between the plains of $CsHSO_4$ crystals?
- Is this transport related to the phase of $CsHSO_4$?
- What is the role of surface diffusion?
- Is H_2 permeance increase due to the proton conductive properties of $CsHSO_4$?

In order to answer these questions, the relation between permeance and the membrane temperature had to be studied (results are given in section 4.4.1). An increasing permeance with temperature could suggest surface diffusion mechanism. A decreasing permeance as a function of the temperature could indicate solution diffusion. Permeance based on Knudsen diffusion will show a decreasing permeance as a function of temperature. Unfortunately, permeance as a function of the pressure could not be performed. The membranes were mechanically not stable enough to withstand any absolute pressure differences. All measurements are based on differences in partial pressure. In section 4.4.4 the proton conductive properties of the membranes and its possible contribution of proton transport towards H_2 permeance are discussed.

4.4.1 Membrane permeance as function of temperature:

Permeance measurements as function of temperature were done at various temperature ranges. The initial temperature range started at 25°C and ended at 180°C. Due to the unexpected permeance results of this experiment, the measurements were repeated with freshly prepared membranes while the highest temperature was reduced from 180°C to

120°C. The membranes were cooled down to room temperature after which the measurement was repeated in triplicate. A third set of experiments was conducted with fresh membranes whereby the temperature cycled between 130ºC and 180ºC. The data of all three temperature ranges are discussed separately in section 4.4.1.1, 4.4.1.2 and 4.4.1.3 respectively.

4.4.1.1 H_2 permeance measurement between 25ºC and 180ºC

H_2 permeance results between 25 and 180°C are illustrated in Fig. 15. It is shown that the H_2 permeance (given in $\mu mol \cdot m^{-2} \cdot s^{-1} \cdot Pa^{-1}$) increases with temperature.

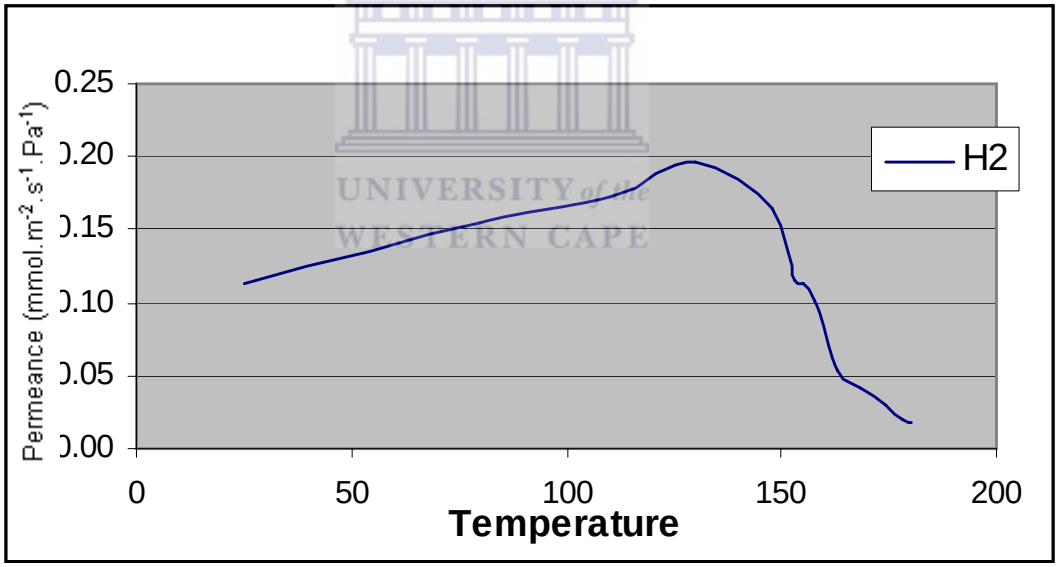

Fig. 15: H_2 permeance as function of temperature (25-180°C)

However when the temperature is raised above 140°C, a sharp reduction of the H_2 permeance is observed. The main question is why an optimal permeance is shown around 140°C. It is known that $CsHSO_4$ exists in various phases. These phases are determined by

external conditions such as temperature, pressure and humidity. The most widely investigated phase is the superprotonic phase, which is formed at 144°C. The permeance results with an optimum around 140ºC indicate a possible relation between the transport mechanism of H_2 through $CsHSO_4$ and the phase in which $CsHSO_4$ exists.

4.4.1.2 H_2 permeance between 25ºC-130ºC

In order to investigate the temperature dependence of the permeance without the interference of a possible phase change, permeance was measured between 25 and 130°C. The H_2 permeance results of 2 freshly prepared membranes are illustrated in Fig. 16.

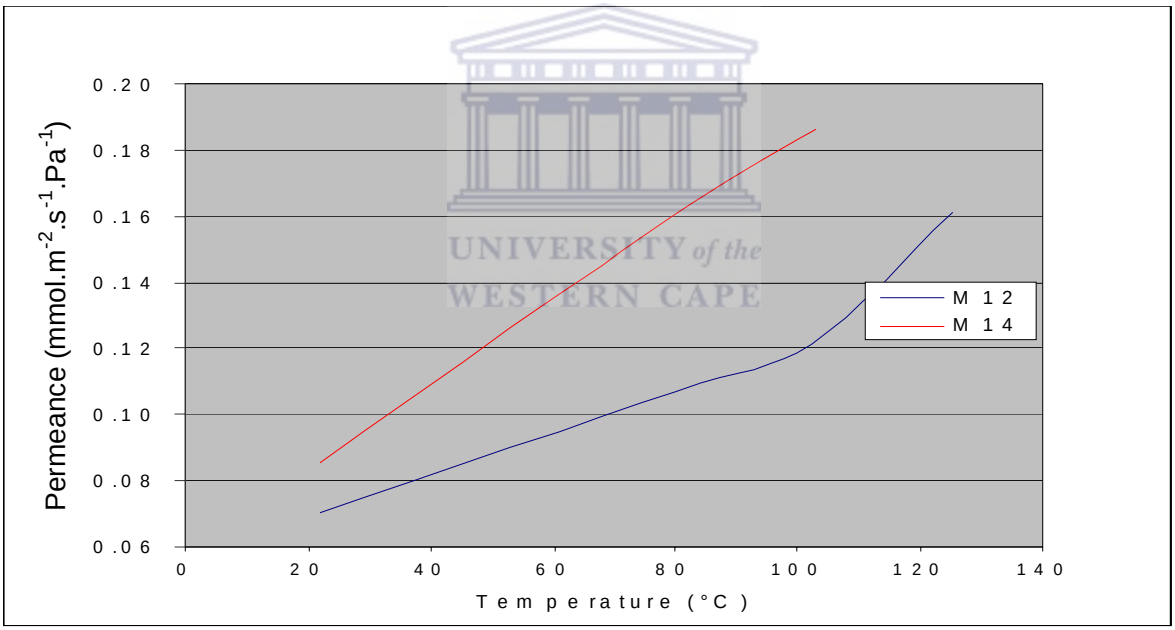

Fig. 16: H_2 permeance as function of temperature (25-130°C)

This figure shows an increase in H_2 permeance as a function of temperature. A mechanism based on surface diffusion will show the opposite effect of temperature. The tested membrane (M12) was cooled down and subjected to another permeance measurement between 20ºC and 130ºC. The results are illustrated in Fig17.

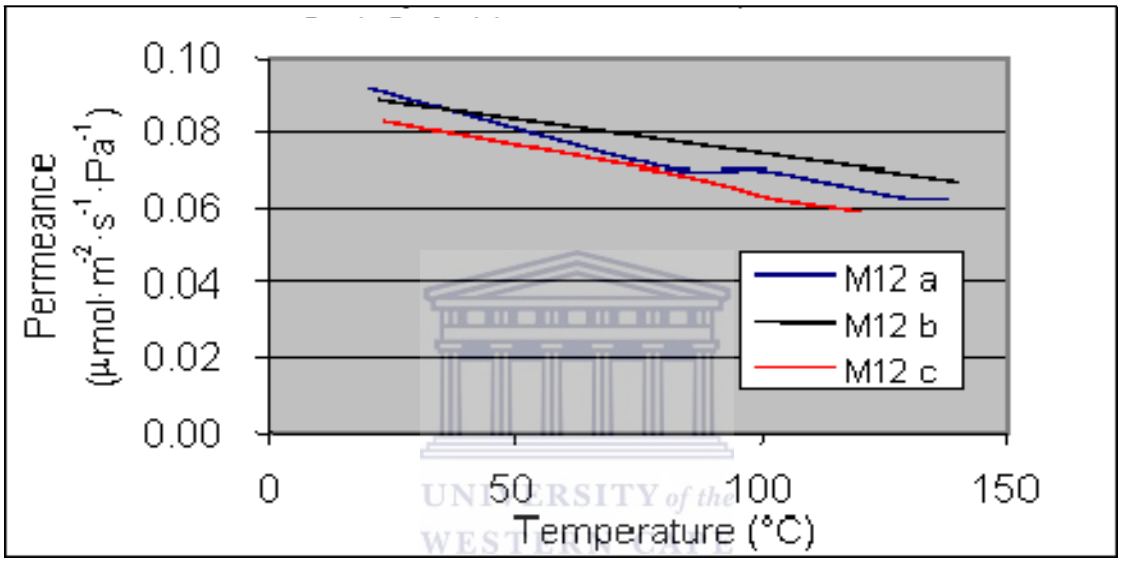

Fig17: H_2 permeance as function of temperature (25-130°C)

This time the permeance decreased as a function of temperature and any subsequent measurement confirmed the same trend. The main question is why the permeance of the membrane initially increases and later decreases with increases temperature.

4.4.1.3 H_2 permeance between 140ºC-180ºC

Fig. 18 illustrates the H_2 permeance of M15 from 140ºC- 180ºC. Starting at 140ºC, the permeance of H_2 decreases as function of temperature. The observed decrease of the permeance possibly means that a phase change in $CsHSO_4$ results in a changing transport mechanism. It may also represent a slow change in the ratio of phases. Between 160ºC and 180ºC sub-lattice melting of the $CsHSO_4$ crystals has been observed before [1]. The formation of an amorphous top layer of $CsHSO_4$ could hamper the H_2 flow. The phenomenon of sub lattice melting has been reported before [1], however not in relation with H_2 permeance.

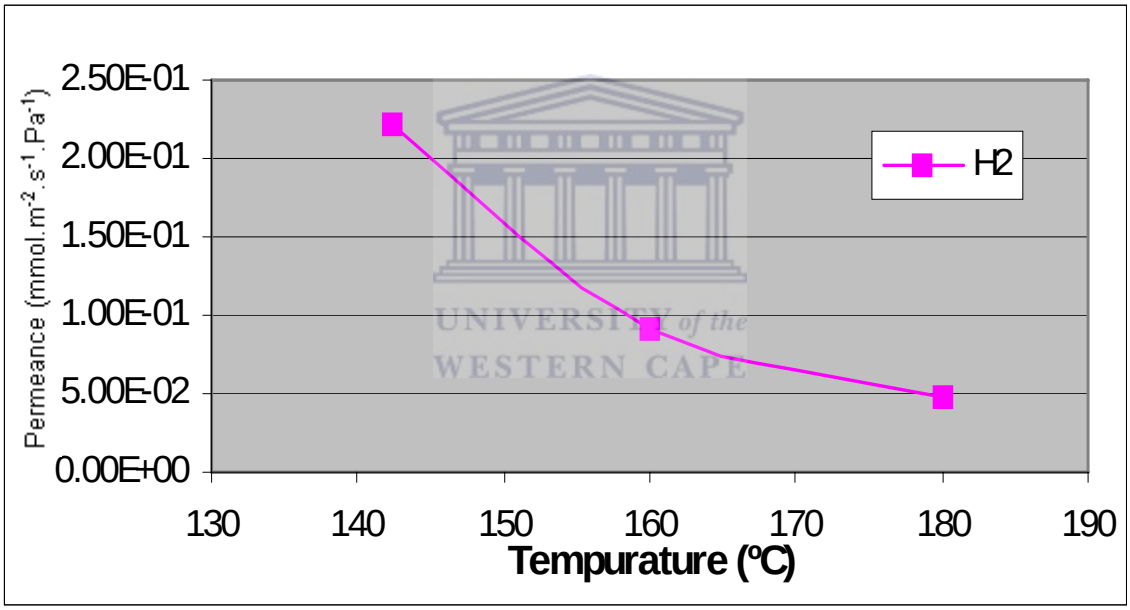

Fig. 18 H_2 permeance as function of temperature (140-180°C)

4.4.1.4 CH_4 and CO_2 permeance between 25ºC-180ºC

The permeance results of CO_2 and CH_4 as function of temperature presented in Fig. 19. It is shown that the permeance is slowly decreasing with increasing temperature. This relation

between permeance and temperature is common when gasses permeate based on the Knudsen diffusion mechanism. The idea selectivity value for CO_2:CH_4 equals 2 at 25°C and becomes 1.7 closer to 180°C. The CH_4:CO_2 separation factor based on molecular sieving would project a factor smaller then 1 since the kinetic diameter of CH_4 is slightly larger than the kinetic diameter of CO_2.

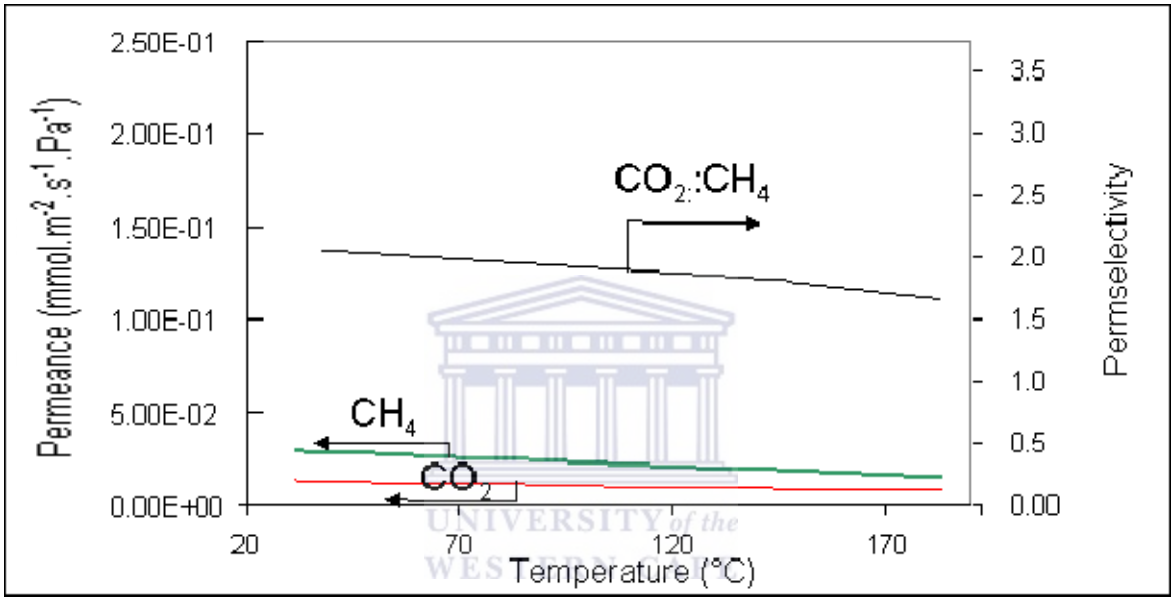

Fig. 19 Permeance and as a function of temperature.

It makes sense to assume that CO_2 and CH_4 travel through Knudsen type of pores (diameter between 0.5 and 2nm), since the theoretical Knudsen separation factor is 1.66. In this case, H_2 will be transported through these pores as well and simultaneously by an additional transport mechanism in order to show higher than Knudsen selectivities.

4.4.2 Phase analysis using XRD

$CsHSO_4$ is sensitive to external condition enforced on the material, transforming from one phase to another [60]. The aim of the XRD analysis is to investigate the relation between the membrane permeance and the $CsHSO_4$ phase change, which is induced by the external condition (temperature, pressure, drying). Unfortunately, the XRD facility did not allow the analysis of the XRD patterns as function of the temperature. All XRD analysis had to be done at room temperature. Note that the XRD pattern of the support did not show any peak between 22 and 32 2Theta. The TGA measurements discussed in section 4.4.3 were used to identify the phase changes as function of temperature. It should be announced that the literature reference used to identify the various phases did not correspond exactly with each other or the sample material. An amalgamation strategy was adopted to analyze the results.

4.4.2.1 Composite:

From the results illustrates in Fig. 20 , the XRD patterns of $CsHSO_4$ (FMA) and impregnated membrane, dried at 80ºC (FMG) are presented.

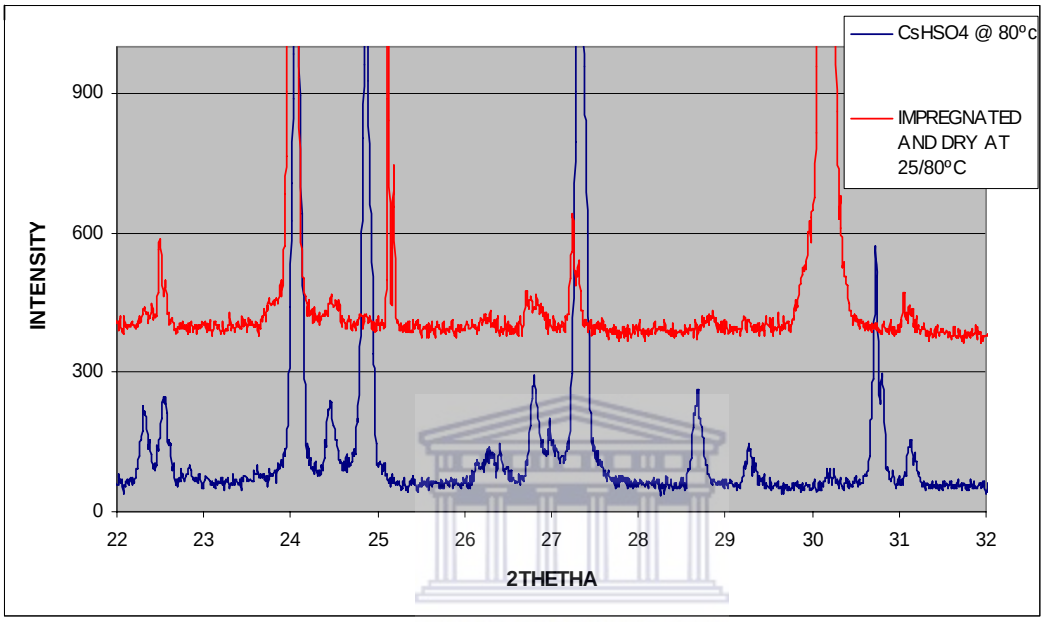

Fig. 20 XRD pattern of $CsHSO_4$ and composite membrane.

The XRD pattern of FMA was introduced to act as a reference. In agreement with Belushkin *et al,* the XRD pattern for FMA corresponds to a mixture of monoclinic structural phases III/II. [60].

4.4.2.2 Phase changes upon exposure to analyte gas:

In this section, it is described that $CsHSO_4$ membranes undergo no phase changes when exposed to analysis gases (H_2, CH_4 and CO_2). From the XRD results presented in Fig. 21, it

is observed that only the intensity of the various peaks is slightly different when comparing the exposed (FMB2) with the unexposed membranes (FMB1)..

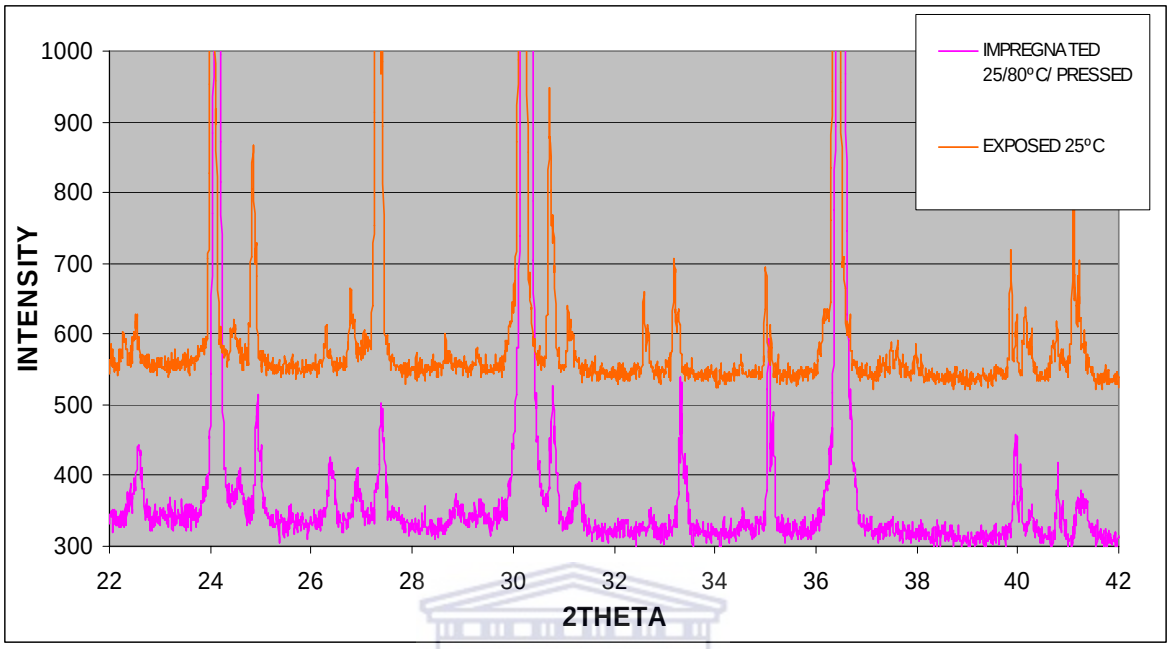

Fig. 21 XRD pattern of $CsHSO_4$ and composite membrane as a function of exposed analyte gases.

The membrane impregnated, dried at 80ºC and pressed, exist in phases II/I and similarly the case for the exposed membrane. This shows that the exposure of the H_2, CH_4 or CO_2 at 25ºC doesn't induce any phase transition within the membrane. With the introduction of $CsHSO_4$ into the glass fibre, the co-existence of phase III and II is observed with a dominant phase II. When $CsHSO_4$ was introduced into the SiO_2 matrix it can be expected that significant parts of $CsHSO_4$ and SiO_2 are present in pure form. Even though some $CsHSO_4$-SiO_2 interface material may exist (on the places were SiO_2 fibre and $CsHSO_4$ meet). The dominance of phase II could be a result of the presents of SiO_2 because the interface material does have a great effect on the stabilization of phases [29].

4.4.2.3 Effect of drying: humidity

The XRD results illustrated in Fig. 22, shows that membranes dried at 25ºC (FME), exist in phase III, where membranes dried at 80ºC (FMG) exist in phase III/II (this sample appears to be more crystalline as well). The peaks representing phase III in the sample dried at 80°C show a slight shift to lower angles which indicates a higher d-spacing. This type of increase in d-spacing may facilitate H_2 transport through the crystal lattice.

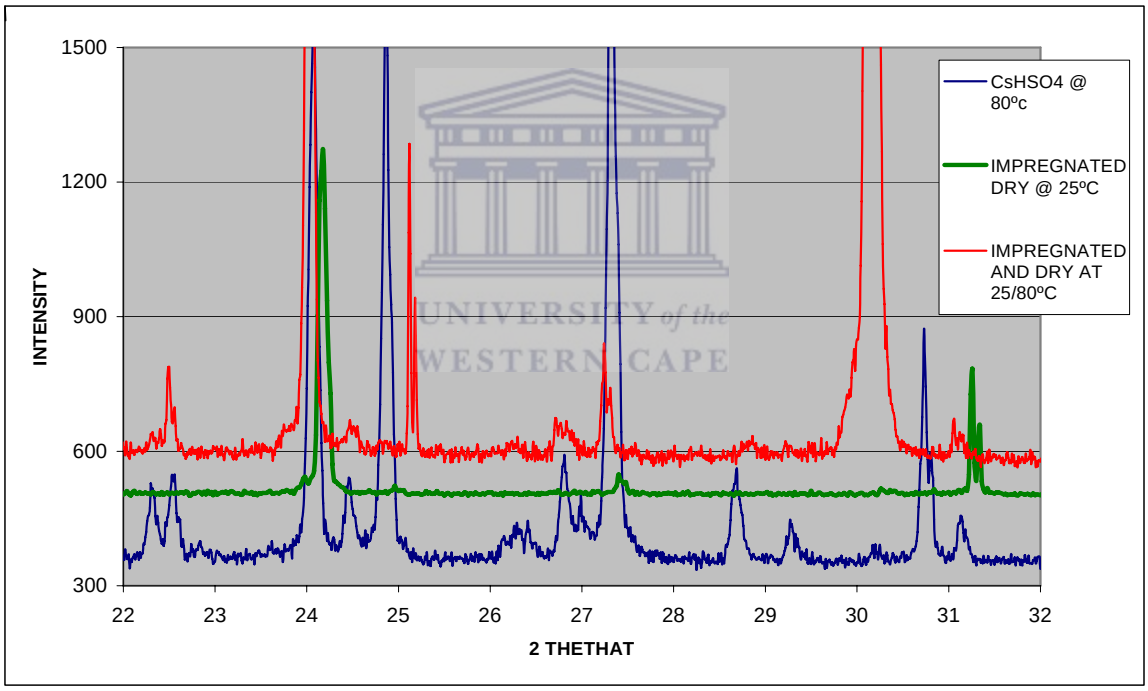

Fig. 22 XRD pattern of $CsHSO_4$ and composite membrane as a function of humidity

4.4.2.4 Effect of hot press:

The XRD results shown in Fig. 23, reveal that $CsHSO_4$ does show a phase change when exposed to uni-axial pressures. Unpressed membrane (FMG) co-exists in phase III/II,

where the pressed membrane (FMB) is transformed from phaseIII/II to phases II/I. This is in accordance to Calum *et al*, $CsHSO_4$ exist or co-exist in phase I (tetragonal space) at 160ºC [16]. It is therefore suggested that the phase induced in $CsHSO_4$ due to the pressing procedure (phase II/I).

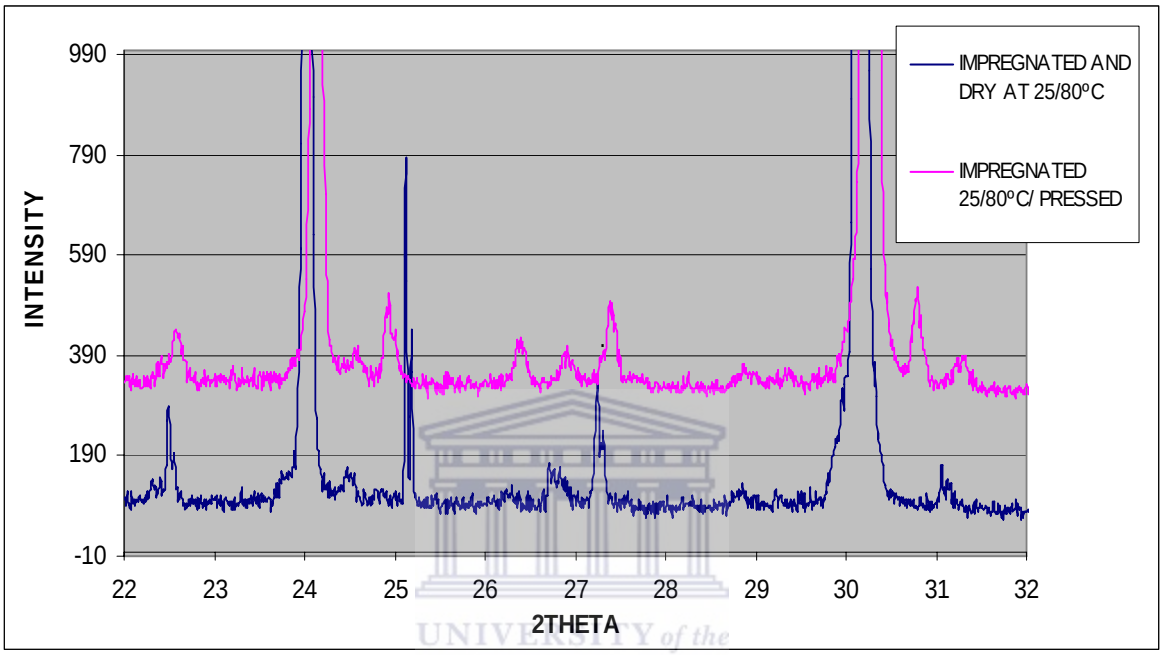

Fig. 23 XRD pattern of $CsHSO_4$ composite membrane as a function pressure

4.4.2.5 Phase changes a result of exposure to increasing temperature:

The membrane (FMB) was subjected to permeance condition at different temperatures and analyzed by means of XRD (as explained, the analysis were done at room temperature).

The XRD diffraction pattern of the membrane exposed at 80ºC (FM3) presented in Fig. 24 shows peaks of phase II. The membrane exposed to 180ºC shows a diffraction pattern similar to the membrane exposed at 80°C. However the membrane exposed to 140° show

a completely different pattern. These XRD patterns show that $CsHSO_4$ can exist in various phases even though all samples were analyzed at room temperature. Please note that peaks shifts are often observed even when the XRD pattern of the samples seem comparable. Unfortunately, no solid conclusions can be drawn since it is not known if any phase change took place upon cooling of the membranes.

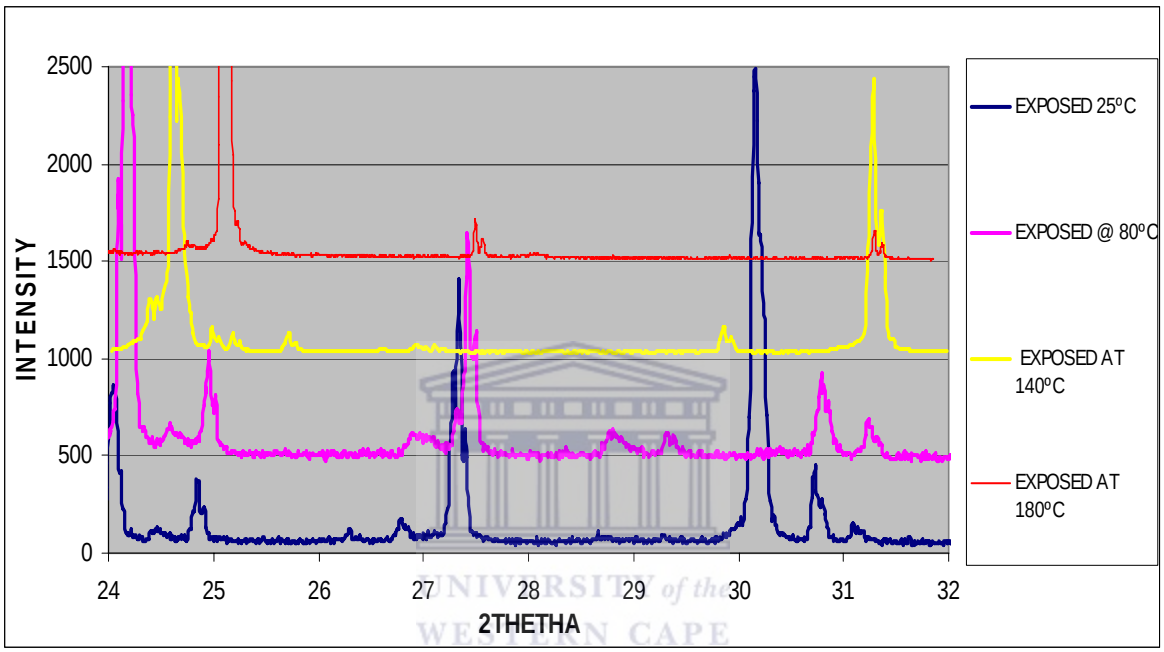

Fig. 24 XRD pattern of $CsHSO_4$ and composite membrane as a function of temperature.

.

4.4.3 Phase analysis using thermal analysis methods:

TGA and DSC are thermal analysis techniques utilized to measure the weight loss and heat flow as a function of temperature and time. The combination of both techniques can give valuable information on phase transitions and decomposition temperatures as well as heat capacity for physical and chemical changes to the sample. As mentioned in section 4.4.2, the XRD facility that was accessible during the course of the project, had an important

limitation since it was not possible to control the temperature of the sample (nor humidity). This shortcoming could partially be resolved by doing TGA. The TGA results will reveal the various phase changes as function of actual temperature. Unfortunately no reference material was found on the heat capacity of the various phase of $CsHSO_4$ so that identification of the phase itself was not possible.

The aim of the investigation is to identify phases of $CsHSO_4$ and its composite membranes as a function of temperature and the effect of SiO_2 has on the bulk $CsHSO_4$.

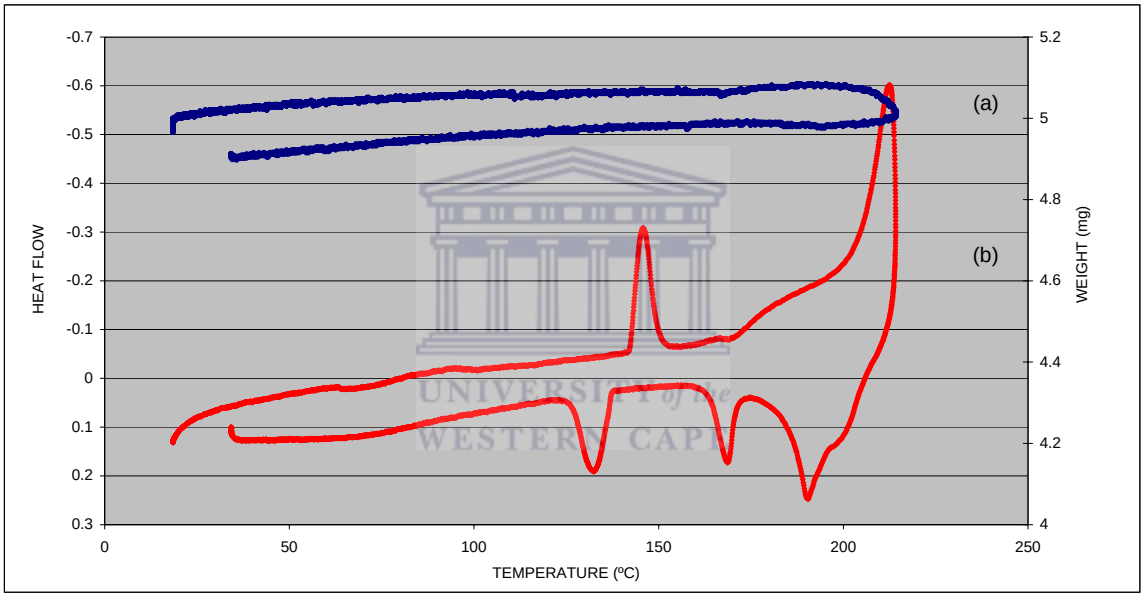

Figure 25 illustrates the TGA (a) and DSC (b) thermal cycle of pure ground $CsHSO_4$ in air.

From the TGA results, the sample weight during the experiment was practically constant which shows that the sample was not oxidized and did not decompose (at least no gaseous or volatile compounds were formed).

With the DSC results, distinct peaks at particular temperatures are presented. The endothermic peak at 146.5°C is most likely related to the formation of the well-studied superprotonic conductive phase of $CsHSO_4$ [29]. From 170 up to 200, a slightly

endothermic peak was observed which might be related to sub lattice melting, which is followed by complete melting of the Sample at 210 °C. The cooling curve suggests solidification of the melted sample at 190-200°C. At 170°C the solidified material changed its phase and at 135°C one again.

The thermal cycle of TGA (b) and DSC (a) analysis on the composite membrane is illustrated in Fig. 26. The insignificant mass loss during the thermal cycle suggests that no decomposition took place which is in agreement with Ponomareva V.G *et al* [63]. The heating cycle of the DSC analysis presents an endothermic peak at 44ºC, which is possibly due to water loss.

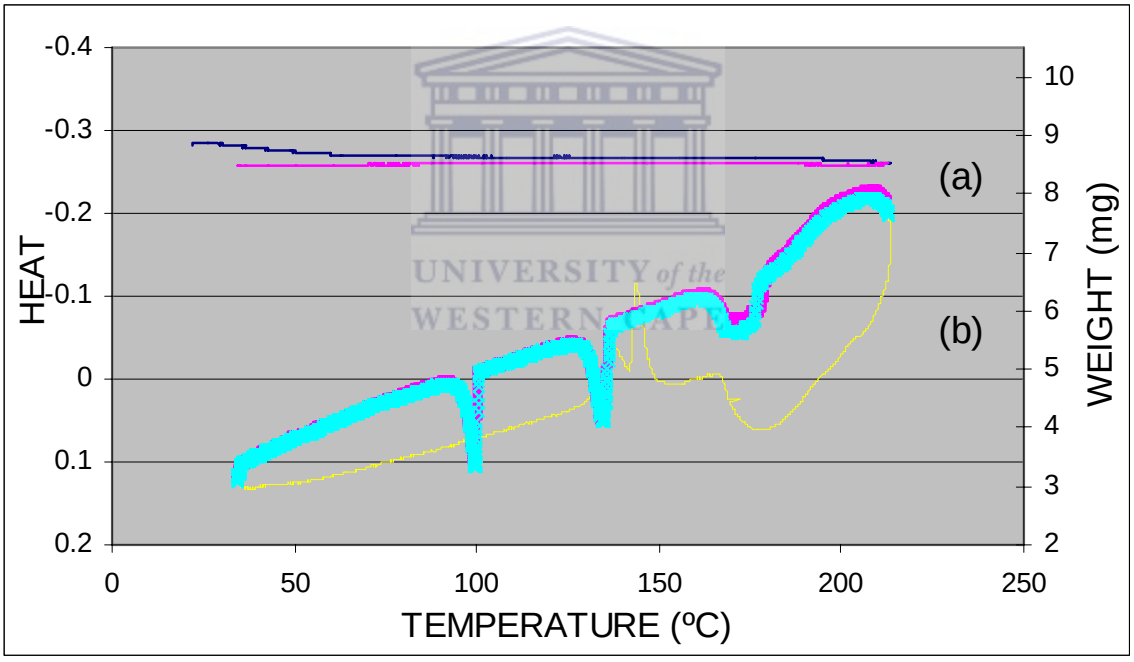

Fig. 26 TGA measurements of thermal cycled $CsHSO_4$ composite membrane

A clear endothermic peak is shown at 145ºC, most likely due to the same phase transition that was observed for the pure $CsHSO_4$. An exothermic peak upon further heating was not

expected and cannot be explained. During the cooling cycle of the membrane sample the exothermic peaks representing the phase change are clearly visible at 170°C, 135°C and 100°C. It seems that all the phase changes occurring during the cooling cycle are all taking place at lower temperature when compared to the transition temperatures for the pure CsHSO4 sample. This finding is in agreement with Ponomarerva *et al*, who observed a retarded shift to lower transition temperatures due to the presents of SiO_2 [63].

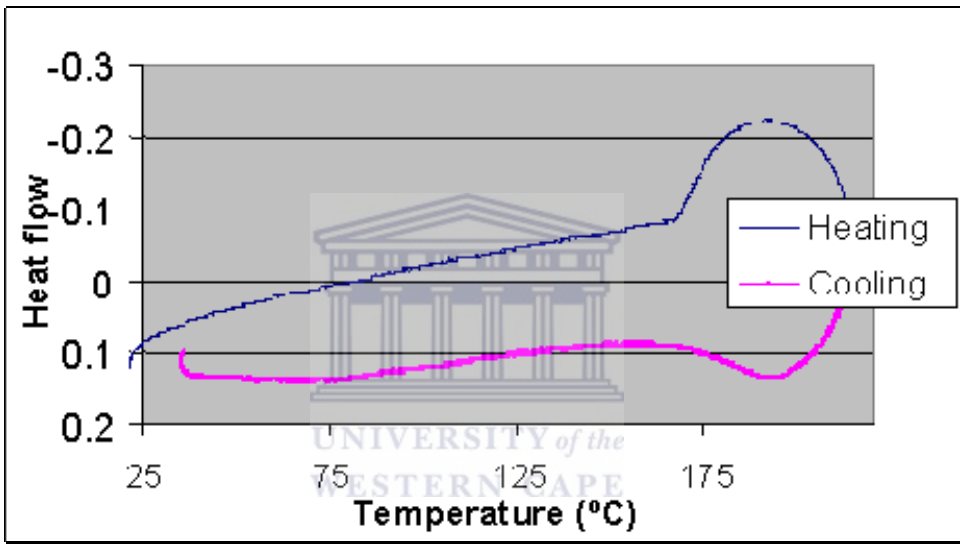

Fig. 27 TGA measurements of thermal cycled glass fibre support

From the DSC results no distinct peaks are evident, however towards the end of a thermal cycle the heatflow shows a strong artefact most likely induced by the change from heating to cooling. This artefact show that care must be taken when interpreting the DSC graph at these temperature regions.

4.4.4 Phase analysis using impedance spectroscopy

As discussed before, there are various mechanisms through which H_2 can diffuse through the membrane. Hydrogen transport via proton conduction is one of the mechanisms. The whole existence of the H_2 fuel cell is based on this principle; H_2 is spit into protons and electrons at one side of the membrane, transported through the membrane in the form of protons and combined with O_2 and electrons to from water.

In this section the proton conductive properties of pure $CsHSO_4$, $CsHSO_4$ membrane and the glass fibre support are discussed. Baranicov *et al* reported that the superprotonic phases for $CsHSO_4$ occur at 140ºC [27]. The change to the superprotonic phase was confirmed by the sudden increase of the proton conductivity when the sample was heated above 140°C as can be seen in Fig. 28. The sudden change in conductivity is a result of the structural change from monoclinic structure that is adopted in phase II (25ºC-130ºC) to tetragonal structure at 140ºC adopted in phase I. This phase change at the same temperature was confirmed by the TGA results in section 4.4.3.

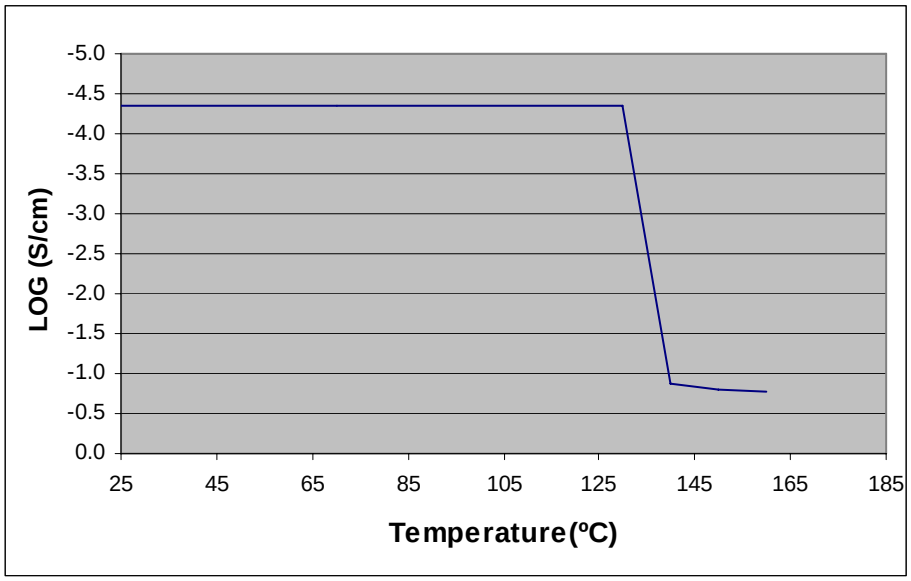

Fig. 28 Proton conduction of $CsHSO_4$

As illustrated in Fig. 29, glass fibre support does not show any conductive properties.

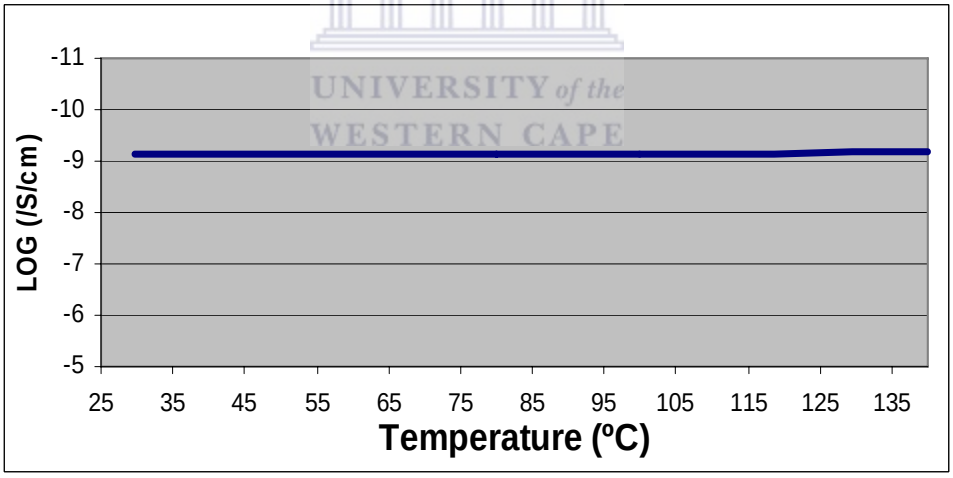

Fig. 29 Proton conduction of glass fibre supports

From Fig. 30, the transition temperature $CsHSO_4$ / SiO_2 decreases in relation to the pure $CsHSO_4$. This is agreement with Shuqiang Wang *et al*, proves SiO_2 significantly lowers the

transition temperature range [26]. This also corresponds to the TGA results in section (4.3.1), which shows a decrease in the transition phase temperature for $CsHSO_4/SiO_2$ as oppose to pure $CsHSO_4$.

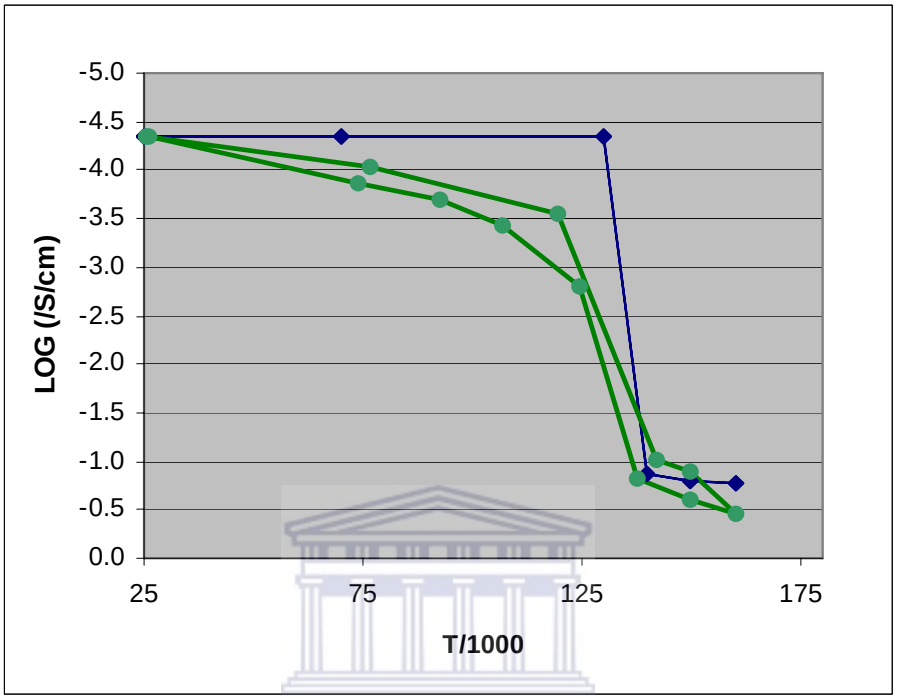

Fig. 30 Proton conduction of $CsHSO_4$ composite membrane

The H_2 permeance results of a $CsHSO_4/SiO_2$ composite membranes (presented in section 4.4.1.3) showed that the H_2 permeance increases as a function of temperature until 135ºC. After this point, a permeance decreases with increasing temperature. It seems that the H2 permeance start to decrease upon formation of the proton conductive phase. The proton conductive phase (phase I) seems less permeable for H_2 than phase II (or II/III). If proton conductivity would be one of the transport mechanisms for H_2, an increase rather than decrease of H2 permeance would be expected when the conductivity increases with 3 order of magnitude.

4.4.5 Summery on transport mechanism

After the various analysis, the following hypothesis can be made around the transport mechanism.

"The gas transport mechanism in $CsHSO_4$ – SiO_2 composite membranes is a combined transport mechanism of Knudsen diffusion and solution diffusion. The pores that allow Knudsen diffusion (allow transport of H_2, CH_4 and CO_2) are believed to be located at the $CsHSO_4$ crystal phase boundaries. In parallel, H_2 diffuses through the lattice of phase II/III of $CsHSO_4$ (or the CsHSO4-SiO2 interface layer)." A schematic representation of this combined transport at 135°C and 180°C is given in Fig 31a and b respectively.

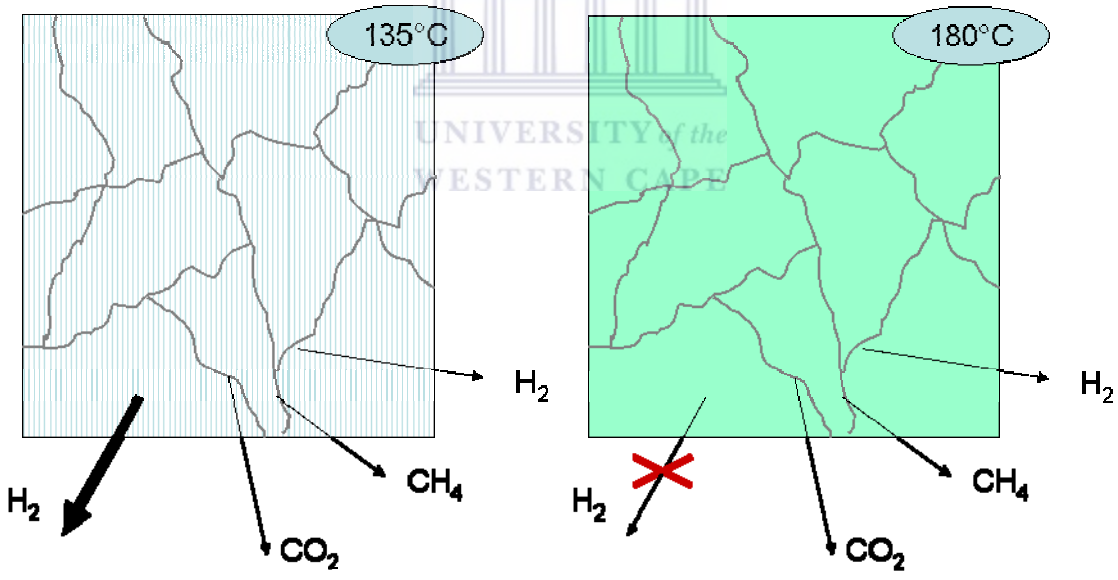

Fig. 31 A schematic representation of the combined transport mechanism in CsHSO4-SiO_2 composite membranes at 135°C (left) and 180°C (right)

The permeance and idea selectivity values of the composite membrane are illustrated in Fig. 32. With the combined transport mechanism one can explain why the permeance and idea selectivity initially increases with temperature. The temperature activated transport of H_2 through the crystal via solution diffusion increases the overall H_2 permeance. At 180°C, when possibly due to sub-lattice melting, the H_2 molecules cannot pass through the membrane by solution diffusion, only through the pores that are also used for CH_4 and CO_2 transport. The selectivities for H_2:CO_2, H_2:CH_4, and CO_2:CH_4 are reduced to 5, 4 and 1.7 respectively which are very close to the selectivities one would expect when separation is based purely on Knudsen diffusion.

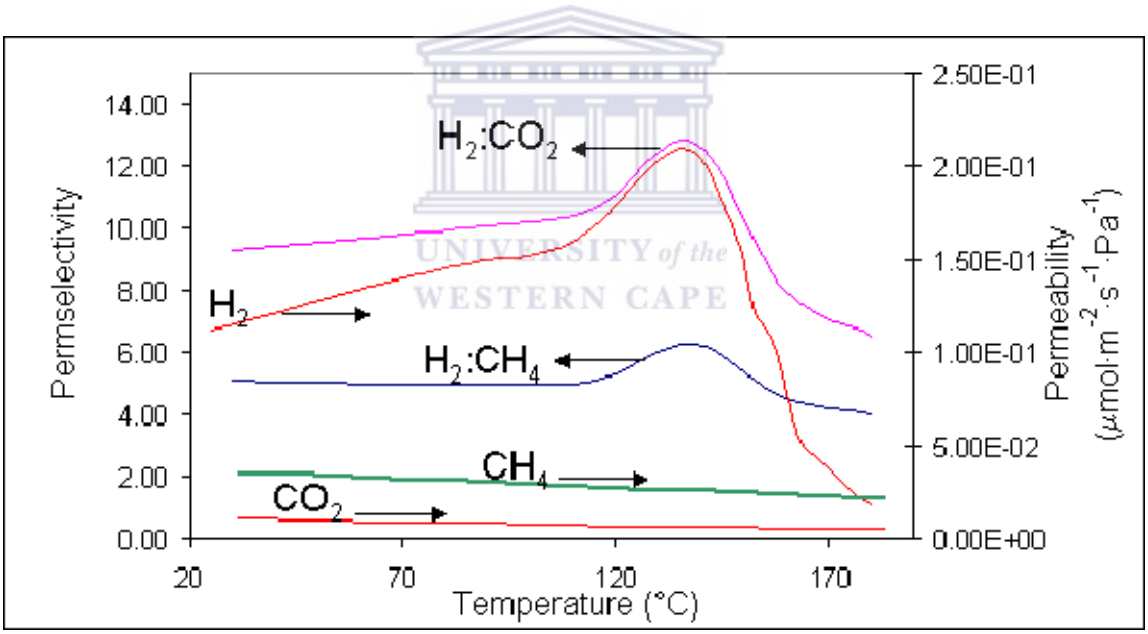

Fig. 32 Permeance and permselectivty as a function of temperature.

Table 4.6 shows that the contribution of solution diffusion towards total H_2 fluxes more of less the same as the flow through the larger pores.

The contribution of the Knudsen diffusion was calculated by multiplying the CO_2 permeance by 4.7. The contribution of the solution diffusion is calculated by subtraction of 0.1-0.047.

Table 4.6: Contribution of Knudsen and Solution diffusion towards total H_2 transport

	Permeance ($\mu mol \cdot m^{-2} \cdot s^{-1} \cdot Pa^{-1}$)			Idea selectivity	
	H_2	CH_4	CO_2	H_2:CH_4	H_2:CO_2
Solution diffusion	0.053				
Knudsen diffusion	0.047				
Total diffusion	0.1	0.02	0.01	5	10

5 CONCLUSION

The following conclusions can be made:

- The preparation procedure for $CsHSO_4$-SiO_2 composite membranes was optimized;
    - The optimal volume of saturated $CsHSO_4$ solution to be impregnated into a glass fibre support was 1ml.
    - The optimal drying temperature prior to the pressing procedure was 80°C for 12h
    - The optimal pressing temperature was found to be 160°C
    - The optimal pressing pressure was 200bar

- Membranes prepared via the optimized procedure showed good reproducibility, H_2 permeance of 0.15 $\mu mol \cdot m^{-2} \cdot s^{-1} \cdot Pa^{-1}$ and a idea selectivity of 5 and 10 towards H_2:CH_4 and H_2:CO_2 respectively

The transport mechanism of gasses through the $CsHSO_4$-SiO_2 composite membrane was studied by gas permeance experiments as function of temperature, TGA and Impedance spectroscopy indicated the formation of the proton conductive phase at 140°C.

- The pores that allow Knudsen diffusion (allow transport of H_2, CH_4 and CO_2) are believed to be located at the $CsHSO_4$ crystal phase boundaries. In parallel, H_2 diffuses selectively through the lattice of phase II/III of $CsHSO_4$The gas transport mechanism is therefore thought to be a combination of Knudsen diffusion and solution diffusion.
- The gas transport mechanism has no significant relation to the proton conductive properties of $CsHSO_4$

6 REFERENCES:

1. Bladergroen B.J (2004), Hydrogen separation, Seminar for department of Chemistry, University of the Western Cape, South Africa.
2. Zittel W, Wurster.R (2001) *Hydrogen in the Energy Sector,* [ONLINE], Available: http://www.hyweb.de/Knowledge/w-i-energiew-eng.html
3. Worrell.E, Phylipsen D (2000) *Energy Use and Energy Intensity of the U.S. Chemical Industry* [ONLINE]
   Available on: http://www.hyweb.de/Knowledge/w-i-energieweng.html
4. Wikipedia (November 2006); *Hydrogen economy*, [ONLINE],
   Available on: http://en.wikipedia.org/wiki/Hydrogen_economy
5. Praxair (2002), Investors trip- Growth in H_2 [ONLINE]
   Available:www.prixair.com
6. Brian l. Bischoff, Roddie R. Judkins, K. Dale Adcock (2002) Development of inorganic membranes for hydrogen separation [ONLINE]
   Available http://www.ornl.gov/sci/fossil/Publications/ANNUAL-2003/imtl.pdf
7. Shivaji Sircar, 2002 Pressure Swing Adsorption *Ind. Eng. Chem. Res.*, *41,* 1389-1392
8. W.C (1998); Permeability of hydrogen in amorphous Pd[(1-x)]Si[x] alloys at elevated temperatures; Journal of Membrane Science 139 29-35
9. Xomeritakis.G (1997), fabrication of thin metallic membranes by MOCVD and sputter, Journal of membrane Science, 133 217-230
10. Bellona foundation (2004) Hydrogen [ONLINE]
    Available: http://193.71.199.52/en/energy/hydrogen/report_6-2002/22852.html

11. G. Naidoo, Cesium Hydrogen Sulphate and cesium dihydrogen phosphate based solid composite electrolyte for fuel cell application, University of Western cape.
12. Mohammad H.S, Chemical Vapor Deposit 3 (6) (1997) 311 317
13. Corrosion-doctors (2005), Metal coat [ONLINE] Available: http://www.corrosion-doctors.org/MetalCoatings/Electroless.htm
14. Membrane technology (2004) [ONLINE] Available: http://www.membrane.nl/serve/theses/matthias/Appendix.pdf.
15. J. Smid a, C.G. Avci b; Preparation and characterization of microporous ceramic hollow fibre membranes, Journal of Membrane Science 112 (1996) 85-90
16. Calum R.I; Superprotonic behavior of Cs (HSO)(H PO) – a new solid acid in the CsHSO –CsH PO system, Material Research Bulletin 35 (2000) 999-1005
17. J.Caro, Noack; Zeolite membranes ± state of their development and perspective, Microporous and Mesoporous ,material 38 (2000) 3-24
18. Chiang. A.S.T; Membranes and films of zeolites and zeolites structures, Journal of physics and chemistry of solids 62 (2001) 1899-1910
19. Sushil Adhikari; Hydrogen Membrane Separation Techniques, Ind Eng.Chem. Res 45 (2006) 875-881
20. Hara S*;* Sakaki K, An amorphous alloy membrane without noble metals for gaseous hydrogen separation Journal of Membrane Science 164 (2000) 289–294
21. Pratibha Pandey and R. S. Chauhan (2001); Progress in Polymer Science 26 (6) 853-893
22. Y.S. Lin (2001); Microporous and dense inorganic membranes: current status and prospective Separation and Purification Technology 25 39–55

23. Kluiters S.C.A (2004) Status review on membrane systems for hydrogen separation, Intermediate report EU project MIGREYD, ECN-C--04-102

24. Roddie R. Judkins, K. Adcock D, Development of inorganic membranes for hydrogen separation, Brian l. Bischoff,. Powell oak ridge national laboratory 2002

25. R Shuqiang Wang; Solid State Ionics 176 (2000) 755-760

26. Shuqiang Wang (2005), Preparation and characterization of proton-conducting $CsHSO_4$–SiO2 nanocomposite electrolyte membranes, Solid State Ionics 176 755–760

27. B.Baranowski (1995); Phase transition of $CsHSO_4$; Journal or Solid state Chemistry 117 412-413

28. J.Baran, Vibrational investigation of phase transitions in CsHSO4 crystal Journal of Molecular Structure 614 (2002) 133–149

29. J. Otomo(2005); Phase transition behavior and proton conduction mechanism in cesium hydrogen sulfate/silica composite, Solid State Ionics 176 755–760

30. B.Yang (2003); Stability of the dry proton conductor $CsHSO_4$ in hydrogen atmosphere, Material Research Bulletin 38 691-698

31. Weber S, Vid K, Cell, Mater. Fus. Med., 28 (1954) 2.

32. https://customer.gewater.com/portalWebApp/saleslocator/sendMailAction.do

33. Xue D, Jing F D (2001); Amorphous Ni–B alloy rceramic composite membrane prepared by an improved electroless plating technique, Materials Letters 47 271–275

34. http://www.hyweb.de/Knowledge/w-i-energiew-eng.html (1996)

35. Bryan D. Morreale; Journal of Membrane Science 212 (2003) 87–97

36. Apel P**S;** Radiation Measurements 34 (2001) 559-566

37. NGUANRUKSA J;Pomer membranes, Polymer testing 23, (2004) 91-99

38. http://en.wikipedia.org/wiki/Sol_gel (2006)

39. Mohammad H.S, Chemical Vapor Deposit 3 (6) (1997) 311 317

40. Dr. D Rajarathnam (2004) Instrumental chemical analysis: Basic principles and techniques;department of chemical biomolecular engineering **1** 12, 22 27.

41. Wikipedia (November 2006); XRD [ONLINE],
Available on: www.wildepedia.com/xrd

42. Uwe T, Olfa K, Characterizing aging effects of lithium ion batteries by impedance spectroscopy; Electrochimica Acta 51 (2006) 1664-1672

43. N.J.G Gardner, S Hull (2006); User Manual for impedence spectroscopy measurement; ruthreford Appleton laboratory 23

44. Wikipedia (November 2006); *SEM*, [ONLINE]
Available on: www.wikipedia.ord/wiki/sem

45. Sergey Vyazokin; Anal Chem 76 (2004) 3299 3312

46. Kok M.V; Thermal Analysis application in fossil fuel science, Middle east technical University; Review paper (2001)

47. J.Czarnecki (2000); Practical thermogravimetry, Journal of thermal Analysis and calorimetry, 60 459-778

48. Seung Eug Nam, Sang Hak Lee (1999); Preparation of a palladium alloy composite membrane supportedin a porous stainless steel by vacuum electrodeposition Journal of Membrane Science 153 163-173

49. Marcel Mulder, Basic Principles Of Membrane Technology 2nd Edition, Kluwer Academic Publishers
50. Grashoff, G.J (1983); Platinum Metal Reviews 27 (4) 157-169
51. Xionghfu Zhang, Haiou Lui (2004); Material Chemistry and Physics 96 42-50
52. R.D Noble,Mei Hong (2004) , Hydrogen Separation through pore size engineered Zeolite membranes, University of Colorado, Department of Chemical and Biological Engineering Boulders,
53. FAIEK MEYER (2005), Preparation and characterization of $CsHSO_4$, Honours UWC.
54. Brian L. Bischoff, Roddie R. Judkins,K (2001); developemnt of the inorganic membranes for hydrogen seperation, Oak Ridge National Laboratory 129-133
55. L.Kirpichnikova; Solid State Ionics 97 (1999) 135-139
56. M. Wessling, A. Bos, M.v.d.Linden, M.Bos, W.E.v.d.Linden, M.H.V. Mulder, Modelling the Permeability of Polymers / A Neural Network Approach
57. http://www.che.utexas.edu/lloyd_group/html_files/People/Patrick%20Hanks.htm
58. Mordkovich. V.Z, Baichtock. Y.K, Sosna. M.H. (1993) The Large-Scale Production of Hydrogen from Gas Mixtures: A Use for Ultra-Thin Palladium Alloy Membranes, *International Journal of Hydrogen Energy*, **18**: 539-544.
59. Bakker. W.J.W. (1999) *Structured Systems in Gas Separation*, Published Thesis, The Netherlands: Delft Technical University.
60. Belushkintl k, Adamst M A, Kolesnikov$q A I and Shuvalovs L A, (1994) Lattice dynamics and effects of anharmonicity in different phases of caesium hydrogen sulphate, I. Phys.: Condens. Matter 6 5823-5832.

61. F. Paulik *(1999)*, Transformation-governed heating techniques in thermal analysis I. Journal of Thermal Analysis and Calorimetry, Vol. 58 711-723

62. Bong-Kuk Sea (1996) Formation of hydrogen permselective silica membrane for elevated temperature hydrogen recovery from a mixture containing steam:SO950-421400020-S

63. Ponomareva V.G (1996); Composite protonic solid electrolytes in the CsHSO,-SiO, system Solid State Ionics 90 161-166

64. Halle S.M, Boysen D.A., Chisholm C.R.I., Merle R.B. Solid acids as fuel cell electrolytes, Nature, 410, 2001

65. Itoh.N, Tomura N; Deposition of palladium inside straight mesopores of anodic alumina tube and its hydrogen permeability; Microporous and Mesoporous Materials 39 (2000) 103±111